Carbon Budget Concept ~~, its Deviations~~ and its Deviation Through the ~~Equation: Climate Economics Perspective~~Pulse Response Lens

Vito Avakumović [1]

[1]Center for Earth System Research and Sustainability (CEN), University of Hamburg, Grindelberg 5, 20144 Hamburg, Germany

Correspondence: Vito Avakumović (vito.avakumovic@uni-hamburg.de)

Abstract. The carbon budget concept ~~is based on discoveries made at the end of the 2000s, claiming that~~ states that the global mean temperature (GMT) increase is roughly linearly dependent on cumulative emissions~~, with a proportionality metric named~~ . The proportionality is measured as the transient climate response to cumulative carbon emissions (TCRE). Since its emergence in natural science, the carbon budget concept has gained prominence as a tool for policymakers and climate economists alike. ~~However, its usage in economic assessments has been critiqued due to its inability to capture time-delay effects and TCRE changing with climatic conditions.~~

In this paper, ~~we define the "perfect budget" equation as a purely linear relationship between GMT and cumulative emissions~~the deviations of the carbon budget and the strict linear relationship implied by the carbon budget are examined. Hereby, ~~we distinguish~~ two sources of deviations ~~from the perfect carbon budget~~are distinguished: emission scenario and climate state dependence. The former stems from the scenario choice, the emission pathway, under the fixed cumulative emissions, and the latter from the change in TCRE with ~~increased cumulative emissions . Introducing~~ changing climatic conditions. Previous literature argues for scenario independence using a stylized set of emission scenarios, and offers a way to fit a non-linear carbon budget equation. This paper tests the full portofolio of emissions using an optimization procedure, showing that deviations stemming from emission pathway choices are less than 10% of the overall temperature increase and gradually diminish, even for extreme scenarios. Moreover, introducing Green's ~~function formalism in the context of the~~ formalism using the temperature response to an emission pulse (hereafter, pulse response) ~~, we provide reasoning behind time delay and possible scenario-dependent deviations and connect~~ as a Green's ~~formalism with the carbon budget equation. Using an optimization program, we show that extreme~~ function, the scenario-dependent ~~deviations are relatively small compared to the overall GMT increase and even smaller when there are no more emissions after the year of optimization. We explain~~ effects were replicated to a high degree. Hence, the behaviour of scenario-dependent deviations can be explained and predicted by the shape of the pulse response. Additionally, ~~we show~~ it is shown that the pulse response changes with climatic conditions, through which ~~we further explain~~ the carbon budget state dependency ~~. Finally, we derive a generalized analytical~~ is explained. Using a changing pulse response as an approximation for a state-dependent TCRE, an alternative method to derive a non-linear carbon budget equation ~~, which captures the state-dependent change of TCRE through a weak exponential GMT increase dependency on cumulative emissions~~is provided. Finally, it is shown how different calibrations of a model can lead to different degrees of carbon budget non-linearities. The analysis is done ~~in FAIRv2~~using FaIRv2.0.0, a simple climate emulator model that includes

climate feedback modifying the carbon cycle~~.~~, along with a one-box model used for comparison purposes. The analysis shows that using the Green's function approach to diagnose a model's carbon budget scenario-dependency, along with the method of deriving the non-linear carbon budget equation, both do not depend on the complexity of the chosen climate model.

1 Introduction

The carbon budget concept, or the carbon budget approach, has gained prominence over the last decade~~for~~, due to its ability to determine allowable carbon dioxide emissions leading to a specific global mean temperature (GMT) increase. In essence, it assumes a direct link between the total cumulative carbon emissions and the temperature increase without the need to know the preceding emission pathway~~, making it both a powerful political and a convenient economic tool~~. Following the concurrent initial discoveries ~~at the end of the~~ in the late 2000s (Allen et al. (2009), Matthews et al. (2009), Meinshausen et al. (2009), Zickfeld et al. (2009)), the concept received wider recognition ~~with its inauguration~~ after being included in the IPCC ~~Fifth Assessment Report in 2013~~[1] ~~(~~AR5 ~~) (Stocker et al., 2013). Over the next 8 years, the carbon budget concept skyrocketed in its significance, such that in the IPCC Sixth Assessment Report (AR6), it arguably takes the main role as a policy recommended~~ WG1 [1] (Stocker et al., 2013), and after being presented as an explicit policy recommendation tool for limiting future climate change ~~, as indicated by its gravity in the summary for policymakers (SPM), chapter D (Masson-Delmotte et al., 2021). To emphasize this claim,~~ in IPCC AR6 WG1 (Table SPM~~.~~2, ~~"~~.2) (Masson-Delmotte et al., 2021), where the 'remaining carbon budgets~~" are identified explicitly – indicating~~ ' indicate how much carbon ~~is left to emit to reach~~ may be emitted while still reaching low-temperature targets, ~~when~~ assuming net-zero emissions ~~afterwards~~afterward. By and large, since its emergence, the carbon budget has become ~~"~~'a staple of climate policy discourse~~":~~ ', having paved the way for various discourses, from policy proposals and international climate justice discussions to financial recommendations and even climate activism arguments for the immediate abandonment of fossil fuels, to name a few ~~(Lahn 2020)~~(Lahn, 2020).

In addition to its ~~substantial~~ policy implications, the carbon budget approach ~~has an ever-increasing relevance~~ plays an important part in the field of climate economics. In the analytic climate economy (ACE) models~~that~~ , which combine general production systems with climate dynamics in an analytically tractable way, the carbon budget approach proves to be a convenient tool that simplifies the analytical approach (Dietz and Venmans, 2019). Since ACE models have a similar structure ~~as~~ to their numerical counterparts, integrated assessment models (IAMs), ~~there is a possibility that~~ the carbon budget approach ~~can make~~ could potentially make the simple climate models used in integrated assessments redundant [2]– if no other non-CO_2 climate change drivers are examined. In decision-making theory, Held (2019) ~~showed that it forms a bridge between~~ has shown that it effectively bridges two decision-making analytic frameworks – cost-effectiveness analysis (CEA) and cost-risk analysis (CRA)~~, the latter being robust under the anticipated climate system learning event~~. The former ~~, alongside the~~

[1] ~~It was not labelled explicitly as a budget but rather presented implicitly through the emphasis on temperature dependency on cumulative emissions (see Figure AR5 SPM.10).~~

[1] It was not labeled explicitly as a budget but rather presented implicitly through the emphasis on temperature dependency on cumulative emissions (see Figure AR5 SPM.10).

[2] ~~That is, if only carbon and no other non-CO_2 climate change drivers are examined.~~

~~cost-benefit analysis (CBA)framework, has been the main tool in IPCC AR5, so~~ is a dominant paradigm in IPCC ARs 5-6, WGIII (IPCC (2014), Shukla et al. (2022)). However, it is dynamically inconsistent when dealing with decision-making under uncertainty and anticipated future learning, as shown by Blau (1974). Held (2019) reasons that the carbon budget ~~approach, along with CRA, de facto saves numerous Working Group 3 results from dynamical inconsistency~~concept, i.e., it being possible to predict temperature solely on the basis of cumulative emissions, is one of the sufficient conditions to retroactively justify CEA-based scenarios as good approximations of CRA-based ones, the latter being dynamically consistent.

Formally, the carbon budget ~~rests on the assumption that the GMT is increasing~~ assumes the GMT increases nearly linearly with cumulative emissions, regardless of the preceding carbon emission scenario. Hence, ~~we define a "perfect budget" equationas follows:~~ a linear carbon budget equation:

$$T(t) = \lambda\Lambda F(t), \tag{1}$$

where $F(t) = \int_0^t E(\tau)\mathrm{d}\tau$ stands for cumulative emissions, and ~~λ~~ Λ is the proportionality constant, ~~named~~ called the transient climate response to cumulative ~~carbon~~ CO_2 emissions (TCRE). The (nearly) linear relationship emerges due to non-linearities ~~counteracting each other~~ cancelling each other out: a concave temperature dependency on the atmospheric carbon content and a convex atmospheric carbon dependency on cumulative emissions (Matthews et al. (2009), Raupach (2013)). The former stems from the radiative efficiency saturation of the atmospheric carbon, the latter from ~~climate feedbacks weakening the~~ the declining ocean heat uptake and the weakening of natural carbon sinks (MacDougall and Friedlingstein, 2015).

~~However, Eq. (1) has been shown to be only an approximation, as the logarithmic effect takes over~~ When it comes to explicitly determining the remaining budget to reach a certain temperature target, a segmented framework had been devised by Rogelj et al. (2018). In essence, it determines what amount of cumulative emissions will lead to a given level of peak warming, if historical, non-CO_2 and Zero Emission Commitment (ZEC) warming are subtracted. ZEC is another metric closely related to TCRE and measures the warming (or cooling) that occurs after emission cessation (Matthews and Weaver, 2010). MacDougall et al. (2020) show that different models perform differently, with an inter-model range of ZEC 50 years following the emission cessation being -0.36 to 0.29 °C. If ZEC were 0, then there would be no time delay in temperature response, and emissions would directly map to temperature according to TCRE. In reality, there is always some time lag between the input and the climate system's response (e.g., Ricke and Caldeira (2014)). Regardless of ZEC, the linear segmented framework concept itself has been challenged by Nicholls et al. (2020), who claim that its assumption of a linear relationship between peak warming and cumulative emissions leads to unrealistically low budgets.

Namely, there is evidence that the relationship between the temperature and cumulative emissions (Eq. (1)) can be non-linear, as either of the two convex or concave mechanisms mentioned above could hypothetically outweigh the other under higher climatic stress (higher T~~and F~~).). Indeed, Gillett et al. (2013) show that the linear relationship overestimates temperature response in most Earth System Models (ESMs). Using the FaIR simple climate model (SCM), Leach et al. (2021) quantify the TCRE drop to approximately 10% per 1000 GtC. Additionally, Leduc et al. (2015) ~~showed~~ have shown that constant TCRE is a good approximation for temperature response under ~~low-intensity emission~~ low-emission scenarios, while it overestimates the model's response to high-intensity scenarios; ~~that reaffirms the necessity~~ this reaffirms the need for TCRE to decrease in

order for the relationship in Eq. (1) to hold true. In this paper, ~~we define and label this~~ the change in TCRE with the changing climatic conditions ~~(higher temperatures & cumulative emissions) as the climate~~ is referred to as (climate) *state-dependent carbon budget deviation*. Furthermore, state-dependent deviations of TCRE lead to a non-linear carbon budget equation, as TCRE is no longer a constant. In the extant literature, Nicholls et al. (2020) have derived the non-linear carbon budget equation by positing a logarithmic relationship between cumulative emissions and temperature increase.

One could imagine a second source of deviation from the budget approach that stems only from the ~~preceding emission scenariochoice~~choice of emission scenario, and not ~~the state~~ from the climate conditions of the system~~; we define and label it as an emission *scenario-dependent carbon budget deviation*. The two introduced carbon budget deviations are inherently independent of each other. The aforementioned state dependence affects the proportionality constant (TCRE) depending on the cumulative emissions F. The emission scenario-dependent carbon budget deviation, however, implies the possibility of achieving a different temperature T following the same amount of cumulative emissions F. The acquired difference can then only depend on the preceding emission scenario choice.~~ . In this paper, this type of deviation is referred to as an *emission scenario-dependent carbon budget deviation*. Previous literature, utilizing the high-complexity climate models (ESMs), ~~argues~~ tends to argue in favour of scenario independency (Gillett et al., 2013). However, the problem with ~~testing~~ using ESMs to study the emission scenario effects ~~with ESMs is that they are computationally costly~~ is that these models are very costly from a computational standpoint, which means only a limited set of ~~stylized~~ emission pathways are examined.~~This problem was tackled by Millar et al. (2016) by~~ Millar et al. (2016) addressed this problem by forcing the simplified, globally aggregated climate model under ~~numerous~~ various emission scenarios. However, ~~we assert that~~ to the best of the author's knowledge at the time of writing, the entire portfolio of emission scenarios that would yield the extreme cases of ~~maximally~~ maximum possible scenario-dependent carbon budget deviations ~~are~~ has yet to be investigated and scrutinized. This paper does so by using the optimization program introduced in Sect. 3.

~~Another often overlooked issue with the carbon budget approach is the absence of its consolidated definition regarding the timescale it operates on . If the carbon budget approach is unambiguously interpreted as in Eq. (1), it would suggest an immediate temperature increase in response to cumulative emissions . In reality, there is always some time lag between the input and the reaction of the climate system. The inability of the carbon budget approach to account for temperature delay was critiqued by Traeger (2021) in the context of ACE. Furthermore, Peters (2018) argues that multiple carbon budgets can be deducted from the same emission scenario~~There is evidence that state- and scenario-dependent deviations are conditional on the model's complexity (MacDougall, 2017), suggesting that models with low linearity have a higher path dependence and vice versa. In this paper, the two effects are approached as separate entities, as the emission scenario-dependent carbon budget deviation implies the possibility of achieving a different temperature T by following a different emission pathway with the same total cumulative emissions F. On the other hand, it is exactly the change in F (and consequently T) that drives the state dependency of TCRE. As will be shown in this paper, in a simple model, one can have one without the other, depending on ~~how the budget is defined~~the model's parametrization.

~~This paper aims~~ At its core, this paper endeavors to define and ~~scrutinize~~ assess both the scenario- and state-dependent deviations (non-linearities) of the carbon budget approach. It demonstrates that a temperature response to an emission pulse, i.e., the pulse response representation, offers a very convenient tool for doing so.

~~We identify the maximally possible~~ The maximum possible and realistic carbon budget scenario-dependent deviations ~~by using the~~ are identified by using an optimization program that maximizes and minimizes temperature in a specific year for fixed cumulative emissions. Through the optimization scheme, the ~~extreme cases are tested; hence, we obtain the upper bound for the scenario-dependent deviations while encompassing the possible time-delay effects simultaneously. We argue that the two effects are interlinked, given that we show that scenario-dependent deviations stem from the time-delayed response of the system.~~ full portfolio of emission pathways is tested.

~~We propose using a temperature response to an emission pulse (e.g. pulse response)~~ Furthermore, a reinterpretation of the carbon budget equation is suggested using a pulse response in the context of Green~~s functionformalism, offering a reinterpretation of the "perfect budget" equation (Eq. (1)), with the idea that it can help to provide the intuition behind the carbon budget deviations. We show that the "perfect budget"~~'s function. It is shown that the linear carbon budget equation is only a special case of ~~Green'~~the Green's function equation. ~~Furthermore, Using the Green's approach~~ More importantly, the paper demonstrates that, by utilizing the pulse response as a Green's function in the above-mentioned optimization program and comparing it to the ~~full-fledged~~ full model results, ~~we confirm its ability to~~ one can capture scenario-dependent effects~~; moreover, its inability to capture state-dependent effects is also revealed .~~

~~With this knowledge, we dive into the causes of the deviations through the lens of the pulse response shape . We show how the shape~~ . Hence, it is revealed that, merely by assessing the shape of the pulse response~~determines possible scenario dependency. Further, we show why the utilization of a non-changing pulse response leads to~~ , one can directly deduce to which extent the model adheres to carbon budget scenario independency. Ultimately, this means that using the Green's function approach allows us to calculate the maximum possible scenario dependency of the ESM models by using their pulse response and running it through the optimization program, which would be otherwise infeasible due to the computational costs.

Lastly, the ~~inability to capture state dependency – since the pulse response shape and magnitude also change over time. Finally, we utilize the fact that pulse response changes with climate conditions to derive the~~ changing pulse response under varying climatic conditions is translated into a state-dependent TCRE. The explicitly quantified state-dependent TCRE is then used to derive a non-linear carbon budget equation, ~~and show that it can emulate the full-fledged modelup to five times higher precision than a regular linear carbon budget relationship.~~ one capable of mimicking the temperature dynamics of the full model. Therefore, it is shown that one can deduce the model's degree of carbon budget non-linearity by examining its pulse response. Further, the scenario independency of the carbon budget approach is confirmed, offering an alternative way of deriving the non-linear carbon budget equation to that put forward by Nicholls et al. (2020).

Overall, this paper ~~aims at an audience from climate economics because it deals with issues that we find vital for that branch: carbon budget , its deviations , and possible utilization of the carbon budget approach in integrated assessments or ACEs. From a natural science perspective, it can be categorized into the body of literature that deals with the conceptual mechanisms behind the carbon budget approach (Raupach (2013), MacDougall and Friedlingstein (2015), Allen et al. (2022)). The difference from~~

the listed literature is that we do not look for is intended for both the climate modeling and climate economics audience. For the climate modeling group, it offers a fresh perspective on how to approach the carbon budget and its deviations through the pulse response lens. Additionally, it shows that the reasoning within the climate model itself, but instead draw conclusions from the output of the modelGreen's function formalism holds considerable potential for predicting the scenario-dependent deviations of complex climate models. For climate economists, it reveals the consequences of using models with incorrect pulse representation, in terms of their inability to adhere to the carbon budget approach.

Following the introduction, the article The paper is arranged as follows. In Sect. 2, we introduce the models and connect Green's framework with the carbon budget equation. In turn, Sect. 3 , we deal deals with scenario dependency. We introduce the optimization procedure The optimization procedure is introduced, followed by the resulting scenario-dependent deviations. In Sect. 4 , we detect the source of the generated deviations through the lens of the pulse response (Green's) function. In Sect. 5, we use the fact that pulse response changes with climatic conditions to derive the state-dependent carbon budget equationdeals with the pulse response representation and its consequences for the carbon budget approach. In Sect. 6, we reflect on the findings and conclude the work5, the findings are discussed in a broader context.

2 Models

This paper utilizes a climate model that includes climate feedback on the carbon cycle. Because we use an optimization procedure The numerical optimization procedure used to generate carbon budget deviations , the requires a substantial number of model runs, so a computationally efficient model has to be chosento be computationally cheap. We will distinguish . Hence, we restrict this analysis to a class of simple climate models (SCMs), also known as climate emulators. We distinguish between and apply two approaches, the full model approach and use two models for inspecting the carbon budget deviation, the full-fledged model and the Green's function model's function approach. While the former is sufficient for inspecting assessing the carbon budget scenario dependencedeviations, the latter mathematically formalizes the carbon budget approach and deepens the offers a deeper understanding of the deviations. The native FAIR language is Python; while in this paper it is incorporated in GAMS . , utilizing the pulse response representation. All of the runs are executed in the GAMS programming language, and the code for all models and runs is available online (https://doi.org/10.5281/zenodo.8314808).

2.1 Full-Fledged FairFaIR model

By the full-fledged model, we mean the FAIRv2FaIR, I am referring to the FaIRv2.0.0 model as prescribed provided by Leach et al. (2021). The model belongs to a class of simple climate models (SCMs), used in integrated assessment models due to their computational affordability. Dietz et al. (2021) suggested it is currently the top choice SCM for climate policy analyses[2] We follow their advice with the Cross-Chapter Box 7.1 in IPCC AR6 WG1 argues in favor of FaIR's value as a climate emulator (Forster et al., 2021). Furthermore, Dietz et al. (2021) recommend employing FaIR in the context of climate economics, a field

[2] They actually argue for the FAIR version 1 given in Millar et al. (2017). However, Leach et al. (2021) argue that the second version is built to emulate the first, with the advantage of being more user-friendly and improved temperature dynamics.

that necessitates the use of SCMs for a previously elucidated reason, namely, computational efficiency. For the purposes of this paper, two features of ~~FAIR being crucialfor this paper~~FaIR are crucial. The first is ~~the above-mentioned~~ its ability to correctly capture the temperature response following ~~one~~ a single carbon emission pulse, i.e. pulse response (Millar et al., 2017)~~. The second feature~~ ; the second is its ability to incorporate climate feedback on the carbon cycle, with one of the effects being ~~a correct representation of change in~~ the modification of pulse response with changing climatic conditions.

In essence, the ~~FAIR model is a~~ FaIR model is an SCM designed to emulate the gas dynamics of different radiative forcers and their effect on the global mean temperature. Because we are interested only in the deviations from the carbon budget, ~~we leave out~~ the non-CO_2 forcers are left out of the analysis, utilizing only the carbon cycle system and its radiative forcing dynamics. The ~~brief modeloverview follows, while the full model~~ model's description and equations ~~are provided in the Appendix~~can be found in Leach et al. (2021).

~~FAIR's carbon cycle~~ In brief, FaIRv2.0.0 consists of four carbon and three temperature ~~boxes (compartments), whose total sum gives the atmospheric carbon concentration inventory and global mean temperature anomalies, respectively. The preindustrial state is equal to all compartments' values set to zero. Each carbon compartment~~ components. Each carbon component has an associated decay timescale which dictates the dissipation of the carbon content into the shared permanent pool that represents the ~~global natural~~ natural global carbon sink. Along with the global temperature increase, the sink~~'~~'s increased content ~~increases~~ creates a feedback mechanism~~. Intuitively, the feedback mechanism mimics the effect of weakening the carbon sinks (absorbing carbon saturates the sinks), while the temperature increase weakens the sinks by, for example, decreasing the carbon solubility in the ocean. With weaker sinks, decay timescales increase, andso does atmospheric carbon~~ , resulting in increased decay timescales and, therefore, increased atmospheric CO2 retention time. The atmospheric concentration gives rise to ~~the~~ radiative forcing by combining a logarithmic and square root term~~. The resulting forcing has the dynamics in temperature boxes equivalent to carbon emissions' dynamics in the carbon boxes.~~ , which translates into the temperature increase distributed between the components. Throughout Sections 3, 4 and 5, FaIR is implemented with its default parametrization, with the default thermal and carbon cycle feedback parameters provided in (Leach et al., 2021), and with the default carbon cycle parameters presented in (Millar et al., 2017).

~~We implement the standard (default) parametrization provided by Leach et al. (2021) for the temperature~~ In Section 6, uncertainty is addressed via a set of six FaIR calibrations. The parameters can be found in Tables 2 and ~~the carbon cycle module. The standard parametrization~~ 3 in (Leach et al., 2021), representing the thermal and carbon cycle feedback parameters tuned to CMIP6 models. Specifically, the sets used in this paper are tuned to the MIROC-ES2L, BCC-CSM2-MR, MPI-ESM1-5, CNRM-ESM2-1, and ACCESS-ESM1-5 models.

2.2 The one-box model

For comparison purposes, another SCM is introduced into the analysis, currently employed[2] as a climate module in the MIND integrated assessment model (Edenhofer et al., 2005). The one-box model consists of only one carbon and one temperature compartment, and it does not include any climate feedbacks. Moreover, Joos et al. (2013) have shown that three to four

[2] It is in the process of being replaced by FaIR

timescales attributed to individual compartments are necessary to correctly approximate the redistribution of CO_2 in the atmosphere. Hence, the one-box model is not sufficient to fully imitate ESMs. Nevertheless, Khabbazan and Held (2019) have shown that different calibrations can be found with which it can emulate the temperature response of ESMs under RCP scenarios. The model's description and equations can be found in ~~the Appendix.~~ Petschel-Held et al. (1999). In this paper, the thermal parameters were chosen to fit the TCR and ECS values provided by FaIR's default parametrization, with the conversion formulae found in Khabbazan and Held (2019).

2.3 ~~Green's Function Framework~~

2.2.1 ~~Green's Function Formalism~~

~~Green's model is, in fact,~~ Note that the one-box model's pulse response should not be considered a correct representation of climate response, but rather a comparison tool. It is introduced in this article precisely because of its inexact pulse response behavior, in order to underscore how the pulse response is connected to carbon budget deviations. Also, it allows us to explore the effects of structural model uncertainty.

2.3 The Green's function framework

2.3.1 The Green's function formalism

Green's model is one equation motivated by the Green's function formalism. ~~In essence~~Essentially, a Green's function $f_{\mathrm{g}}(t-\tau)$ is a specific function unique to a set of linear differential equations $Lx(t) = y(t)$, where $y(t)$ is the input forcing and $x(t)$ is the state variable that changes according to the forcing and the linear operator L. The advantage of Green's function is that it acts as a ~~"propagator"~~ 'propagator' from the input variable (external forcing) to the output variable (change in state variable)~~in such a way that it is possible to circumvent the~~ , allowing us to replace differential equations with just one equation~~that~~ , which reads as $x(t) = \int_{t_0}^{t} y(\tau) f_{\mathrm{g}}(t-\tau)\mathrm{d}\tau$.

Using the same formalism, ~~we propose~~ Green's equation is proposed in the context of global mean temperature dynamics ~~. We are interested in inspecting the temperature dependence on the emission pathway, where the latter and former take the abovementioned role of input and output variables, respectively~~with a climate model in lieu of a set of linear differential equations (see Raupach (2013)). Hence, we propose the following equation~~imitating~~ , imitating the Green's ~~equation~~ function formalism:

$$T(t) = \int_{t_0}^{t} E(\tau) f_{\mathrm{g}}(t-\tau)\mathrm{d}\tau. \tag{2}$$

The output variable is the global mean temperature change $T(t)$, and the input (forcing) variable is the emissions $E(t)$. Green's function ~~$) f_{\mathrm{g}}(t-\tau)$~~ $f_{\mathrm{g}}(t-\tau)$ modifies the contribution to a current temperature $T(t)$ ~~,~~stemming from the ~~emission in the past~~ past emissions $E(\tau)$. According to Eq. (2), the temperature in time t will depend on each emission contributing at time τ prior to t, with the effect modified ~~with~~ by Green's function f_{g} dependent on how far the emission year τ is from t , hence

$f_g(t-\tau)$. Essentially, it is an integration scheme that counts the temporarily modified temperature contributions ~~of~~ to each emission pulse, going backwards from moment t, with a temperature being a superposition of modified contributions. Similar approaches can be found in the literature in Shine et al. (2005) and Ricke and Caldeira (2014). The difference is that, in Eq. (2), the temperature is deduced directly from emissions, without the need for quantifying the radiative forcing and/or atmospheric CO_2 response. ~~Hence, it captures the time delay effects of translating emissions to temperature change.~~

2.3.2 ~~Pulse Response~~ The pulse response as Green's ~~Function~~function

To ~~use~~ make use of Eq. (2), one must opt for a shape ~~of a~~ matching Green's function f_g. Following the proposed definition, we choose it to be a temperature evolution response following the 1 GtC emission pulse, or simply, the ~~"pulse response"~~'pulse response'. Therefore, in this paper, the terms ~~"~~'Green's function~~", "pulse response" or "~~', 'pulse response', and 'temperature evolution following the emission pulse~~" all have the same meaning~~' are interchangeable. Pulse response experiments are one of the generic experiments ~~when inspecting~~ applied when evaluating climate models. ~~We follow the traditional way~~ Following the literature (Joos et al. (2013), Millar et al. (2017))~~of generating~~ , the pulse response is generated by adding a ~~pulse on top of a constant~~ unit emission pulse on prescribed emissions that keep a constant background atmospheric concentration background[3]~~.~~

~~In previous literature, authors have tested the pulse response following the 100 GtC emission injection. Compared to its 100 GtC counterpart, the qualitative shape of the pulse response stays the same for a 1 GtC injection, with the magnitude scaled down accordingly. Generating the pulse response (Green's function) is done by utilizing the full-fledged FAIR model, ~~, as follows.

~~Until 2020, the full-fledged model was forced by~~ The model is forced by the idealized RCP6.0 ~~carbon~~ CO_2-only emission scenario provided by the RCMIP protocol (Nicholls, 2021), starting from the ~~preindustrial era. In 2020, the model concentration level of 402 ppm is reached and, from that year, kept constant, while the emissions~~ year 1850. In the year of pulse response generation t_p, the emission pathway necessary to keep ~~that concentration level unchanged are diagnosed. One advantage of the GAMS programming language is that it allows this procedure without rearranging equations, as is necessary for Python (the original language of FAIR model). Instead, we change the role of emissionsand concentrations from input to output variables and vice versa. After the emissions required to keep the concentration constant are generated, we run two experiments from the year 2020: one~~ the level of atmospheric concentration $C_a(t_p)$ constant is generated. Using the derived emissions, two experiments are run: One with the generated emissions only and one with 1 GtC extra added in ~~2020. Thus, t_p~~. Thus, the pulse response (Green's function) is ~~generated~~ determined by subtracting the temperature evolution of the two runs.

The pulse response functions generated for different years (and hence, different climatic conditions) can be found in Figs. 1a, 1b, and 9, for the FaIR model standard parametrization, one-box model, and different FaIR parametrizations, respectively.

The Green's ~~function~~ functions f_g ~~generated in such a manner,~~ utilized in Green's model (Eq. (2)) ~~, is depicted in Fig. 4 in blue (labelled as Green1.~~ are generated at the year $t_p = 2020$ and depicted in blue (pulse2020) in Figs. 1a and 1b.

[3] ~~One possible way would be adding an emission pulse on top of a prescribed emission pathway.~~

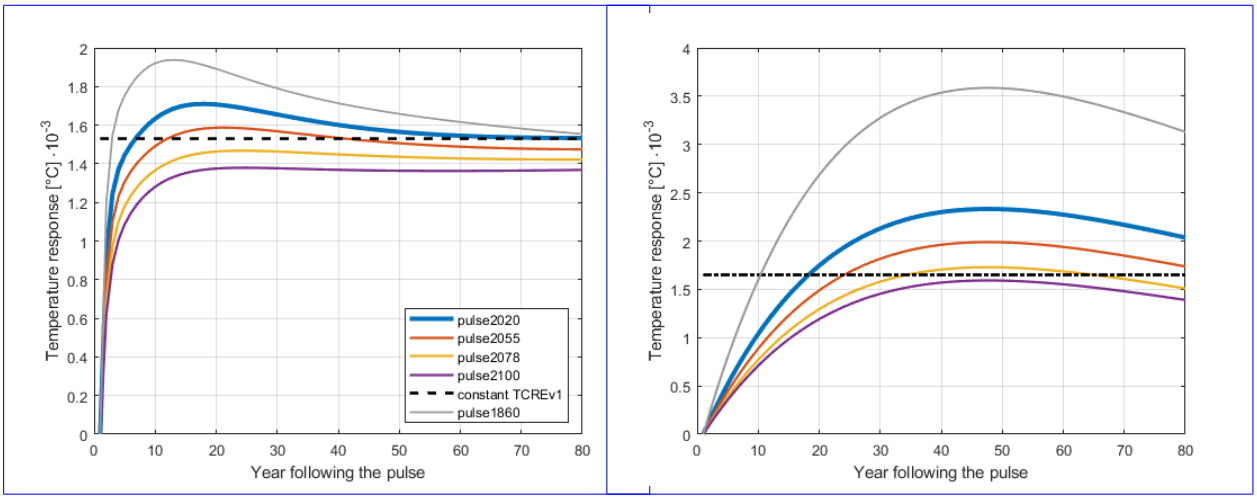

(a) Default parametrization FaIR (b) One-box model

Figure 1. Temperature evolutions in response to 1 GtC emission pulse for different climatic conditions, i.e., pulse responses (colored lines), and the temperature response implied by Eq. (1) (black dashed line). The numbers correspond to the year of an idealized RCP6.0 scenario in which the pulses were generated. Years 2020, 2055, 2078 and 2100 correspond to the FaIR generated background temperatures of 1, 1.5, 2 and 2.5 °C, respectively, and 1860 to preindustrial climatic conditions. Constants TCREv1 and TCREv2 are equal to 1.53 and $1.6 \cdot 10^{-3}$ °C GtC^{-1} and correspond to the central TCRE estimates in Leach et al (2021) and AR6, respectively.

2.3.3 ~~Carbon Budget Equation~~ The carbon budget equation in the ~~Context~~ context of Green's ~~Formalism~~formalism

Next, ~~we inspect~~ the connection between Green's function (Eq. (2)) and the carbon budget suggested by Eq. ~~1.~~ (1) is examined. As a first test of Green's approach, ~~we show that the "perfect budget" equation is just~~ it is shown that the linear carbon budget equation is merely a special case of the former. ~~Furthermore, the viability of Green's approach is numerically tested in the next section, compared to full-fledged FAIR in the context of scenario-dependent deviations.~~

Essentially, the ~~"perfect budget"~~ linear carbon equation suggests an immediate temperature response to (cumulative) emissions, and that ~~that~~ said response does not change in time or with climatic conditions. ~~That~~ This implies that the pulse response introduced in the previous subsection should also be a constant function. In Fig. 41, it is plotted ~~in~~ as a dashed black line~~: the temperature response to an emission pulse has an immediate jump following the emissions, and it does not change in time, as the "perfect budget" implies.~~

~~.~~ Formally, a ~~"perfect budget" temperature~~ linear budget pulse response can be interpreted as a Heaviside function $\Theta(t)$ multiplied by a constant ~~. If the carbon budget framework is consistent, it has to be equal to TCRE. Hence, we set it equal to the central estimate of TCRE from Leach et al. (2021), $\lambda = 1.53 \cdot 10^{-3}$ °C GtC^{-1}. With that, we propose the "perfect budget"~~

temperature response f_g^0 to have the following mathematical form: equal to Λ representing TCRE:

$$f_g^0(t-\tau) = \lambda\Lambda\Theta(t-\tau) = \begin{cases} 0 & t < \tau \\ \Lambda & t \geq \tau \end{cases}, \tag{3}$$

where τ is the timing of the emission pulse and is equal to the 0th year in Fig. 4. Clearly, there is no temperature response before the pulse; therefore, the Heaviside function has a momentary jump in the time of the emission pulse. 1.

Now we show that Proving that the Green's formalism can be considered an analogue to the carbon budget approach . We assume the "perfect budget " temperature response (Eq. (1)) as a is simple. Inserting the idealized budget Green's function and insert it into the Green's equation (into Eq. (2)), and then the claim is easily proved:

$$T(t) = \int_{t_0}^{t} E(\tau) f_g^0(t-\tau)\mathrm{d}\tau = \int_{t_0}^{t} E(\tau)\lambda\Theta(t-\tau)\mathrm{d}\tau = \lambda \int_{t_0}^{t} E(t')\mathrm{d}t' = \lambda F(t).$$

, one arrives precisely at the linear budget equation (Eq. (1)):

$$T(t) = \int_{t_0}^{t} E(\tau) f_g^0(t-\tau)\mathrm{d}\tau = \int_{t_0}^{t} E(\tau)\Lambda\Theta(t-\tau)\mathrm{d}\tau = \Lambda \int_{t_0}^{t} E(t')\mathrm{d}t' = \Lambda F(t).$$

The derived equation is precisely the carbon budget equation , as given in the introduction. We can conclude that Therefore, if the temperature response always had the same (constant) shape as the dashed line in Fig. 41, the carbon budget would have deviations and no time delay – show deviations – each unit of carbon emission momentarily adds would immediately add to the warming equally , and regardless of when it was emitted.

However, as shown in Fig. 4, the FAIR-generated pulse response (blue line) is 1, the FaIR-generated pulse responses are not a constant function. Hence, Eq. (1) does not perfectly hold, and , a fact that has implications for the carbon budget deviations, as will be shown.

In conclusion, Eq. (2) can is to be interpreted as a generalized carbon budget equation . Because of the (non-constant) shape of the generated pulse response, Eq. (2) generalizes the carbon budget equation in a way that enables time-delay effects that lead to possible emission scenario dependencies. The following section will test Green's framework against the full-fledged model. Furthermore, Sectthat allows the deviations. Sects. 4 thoroughly scrutinizes and 6 thoroughly scrutinize the connection between the pulse response shape and possible carbon budget scenario-dependent deviations.

Before going further, we briefly go back to the formalistic introduction of Green's framework from the aspect of carbon budget state-dependent deviations. By proposing carbon budget deviations. In the following section, the viability of Green's approach (Eq. (2)and using FAIR-generated Green's function, we assume that FAIR is a set of linear differential equations. This is false because non-linearities arise in the carbon cycle through the climate feedback parameter and in the logarithmic dependence of radiative forcing on atmospheric concentration. This effectively means that while Green's function can capture time-delay effects, it cannot capture the effects of climate state change on the carbon budget approach. The effect is visible

~~when comparing full-fledged and Green's model optimization runs with higher cumulative emissions. Nevertheless, Sect. 4 shows how state dependency can be detected through the changing pulse response. Hence, pulse representation helps us understand changing TCRE with climatic conditions and, finally, derive the new, reinterpreted carbon budget equation that captures state-dependent~~) is compared to its respective model in the context of scenario-dependent deviations.

3 ~~Scenario-Dependent Deviation~~Scenario-dependent deviation

3.1 Method

3.1.1 Minimization/Maximization ~~Scheme~~scheme

To test the possible scenario-dependent carbon budget deviations, the optimization program is formulated as follows:

$$\underset{\{E(t)\}}{(\mathrm{Max},\mathrm{Min})}[T(t^*)] \quad \text{s.t.} \int_{t_0}^{t^*} E(t)\mathrm{d}t = F_{\mathrm{tot}}, \left|\frac{\mathrm{d}E(t)}{\mathrm{d}t}\right| \leq k,\, E(t) \geq 0,\, E(t_0) = E_0. \tag{4}$$

~~Using the full-fledged and Green's model independently, the~~ The program maximizes (minimizes) the temperature variable in a given ~~specific~~ optimization year t^*. The ~~generated minimal~~ minimum $T_{\mathrm{min}}(t^*)$ and ~~maximal~~ maximum $T_{\mathrm{max}}(t^*)$ temperatures generated provide the upper and lower ~~bound~~ bounds for possible temperatures under the given constraints, elaborated on in the following paragraphs. The ~~maximal~~ maximum possible scenario-dependent carbon budget deviation T_{d} is then calculated by subtracting the two boundary temperatures, $T_{\mathrm{d}}(t^*) = T_{\mathrm{max}}(t^*) - T_{\mathrm{min}}(t^*)$.

In the optimization program (Eq. (4)), the emission pathway ~~takes~~ assumes the role of the free control variable, except in the fixed initial condition $E(t_0) = E_0$. Hence, the novelty of testing ~~the~~ scenario independence with the optimization program is that the emission pathway is generated, instead of being assumed as an input by the user. This way, the analysis does not rely on a limited number of emission scenarios but systematically runs through the whole portfolio of possible scenarios under given constraints. To both avoid trivial solutions and keep the generated emission pathways within what ~~we deem as~~ is deemed realistic, three boundary conditions are implemented.

The first boundary condition sets the total cumulative emissions at the year of optimization t^* to a fixed value F_{tot}, counting from the initial year t_0, chosen as the year 2020 in RCP6.0. The condition ~~restricts the emissions from diverging by keeping them within realistic boundaries. More importantly, it~~ on F_{tot} ensures that the deviation from the carbon budget stems only from the difference between the emission pathways~~(~~, as it fixes the cumulative emissions to be equal at the end of both the minimization and ~~maximization run). In our experiment, the chosen F_{tot} values are 416, 600, 800, and 1000 GtC. The first one (416 GtC), in addition to historical cumulative emissions, amounts to 1000 GtC since the preindustrial era, which approximately corresponds to the carbon budget of keeping the global mean temperature below 2°C with 67% probability, as suggested by the IPCC report (Masson-Delmotte et al. (2021), Table SPM.2). In our run, however, 2 °C will not be reached with those cumulative emissions since the effects of other non-CO_2 radiative forcers are left out. Other values for F_{tot} are chosen generically to test the effect of higher cumulative emissions on scenario-dependent deviations.~~ the maximization run.

The second boundary condition ~~gives~~ provides the upper bound on the rate of change ~~of~~ in emissions per year, effectively setting the allowed absolute slope of the emission pathway to be less than or equal to a prescribed value k. Hence, a trivial solution (e.g., emitting all of the emissions in one year) is avoided. ~~Furthermore,~~ The emission slope k is ~~chosen in a way to be politically relevant. It is restricted to have~~ restricted to the upper bound of 1 $\mathrm{GtC/yr^2}$, roughly corresponding to the emission reduction rate if the annual emissions were linearly reduced to zero between the years 2020 and 2030.

The combination of the restriction on k with the F_{tot} restriction will affect the run's feasibility. The higher the cumulative emissions and the lower the k is, the less ~~likely~~ feasible the run is~~feasible. We can easily visualize that if we keep in mind that cumulative emissions are the surface area below the emissions path. First, remember that we start the optimization in the year t_0 with the corresponding fixed initial emissions E_0. Now, let us assume that we want to reach some F_{tot} at the year t^*; we can immediately conclude that $k = 0$ is feasible for only one combination of E_0, t^* and F_{tot}, that is: $F_{\text{tot}} = E_0(t^* - t_0)$. If we additionally require that we reach~~ . Moreover, the additional requirement that the emissions reach net-zero by t^* ~~, the run becomes infeasible since there ought to be a slope to reach that goal. If we allow the emissions to increase (decrease) fast enough with a larger k value, the run becomes feasible again (for fixed F_{tot}).~~

~~Additionally, the~~ further negatively affects the feasibility. The feasibility limiting value of k will correspond to the run where both $T_{\text{max}}(t^*)$ and $T_{\text{min}}(t^*)$ are equal, as they come from the only possible and feasible scenario; hence, the scenario-dependent carbon deviation $T_{\text{d}}(t^*)$ is zero for that specific k. ~~This is to be expected since for the limiting value of~~ The higher k ~~, only one emission pathway is~~feasible under the ~~specified~~ F_{tot}. ~~Therefore, only one emission pathway can be generated, equal for the minimizer and the maximizer. Following the same logic, if we are slightly above the limiting k, the deviations will always be small, regardless of other variables (e.g. F_{tot}). With the higher k, the~~ is, the more the range of possible pathway combinations increases, ~~and so~~ as does T_{d}.

The last boundary condition ~~does not allow for~~ excludes negative emissions. ~~While there are certain indications that they ought to be employed to meet low-temperature targets, it is unclear how well FAIR fares with negative emissions and if it makes sense to use the model for that purpose~~This condition is utilized since Green's approach uses a pulse response generated under positive emissions. Nevertheless, for the sake of completeness, negative emissions will be allowed in the last part of the section to see how doing so affects the deviation in FaIR.

3.1.2 Two ~~Cases~~ settings of ~~Carbon Budget Interpretation~~the scenario-dependent deviations

To ~~add another layer to the discussion on how the carbon budget can be interpreted~~examine the carbon budget interpretation, we distinguish ~~two additional cases~~ between two additional sets of conditions that differ depending on how much we emit after the ~~time of interest (in our case~~ optimization year (t^*).

~~We address the~~ The first carbon budget interpretation ~~as a "~~is addressed as a net-zero budget ~~"~~ case, which corresponds to the situation in which all of the carbon has been emitted up until the ~~time point~~ point in time of interest, and there are no other emissions ~~afterwards~~afterward. This interpretation coincides more with a carbon budget ~~in a literal sense of budget, which states how much carbon is left in-store for~~ as addressed by the IPCC, which indicates how much more carbon can be emitted while still reaching specific targets. ~~Henceforth, we attribute it to the policy-relevant domain.~~ In the corresponding emission

scenario set, the emissions are bound to reach zero by the year t^* and stay zero from there onwards ($E(t \geq t^*) = 0$). Note, however, that this is not the case of calculating the ZEC deviations, even though the requirement is emission cessation. ZEC tells us what the temperature evolution will be following emission cessation. In the optimization program, however, one derives two maximally different possible temperatures in a specific year, stemming from different preceding emission choices, and the deviation comes from deducting the two. ZEC affects both boundary temperature cases equally, so when the two are subtracted to get the deviation $T_d(t^*)$, the effect of ZEC is also subtracted.

~~On the other hand, we can distinguish the so-called "open budget" case . In this case,~~ On the other hand, there is the transient budget case, in which only the ~~net-zero requirement at the year of interest does not need to be fulfilled, as we are only interested in the~~ momentary relationship between the current cumulative emissions and current temperature increase is of interest; the emissions can evolve freely after t^*. This interpretation can be attributed to the carbon budget approach, as seen through the lens of climate economics~~through the instantaneous relationship between temperature and cumulative emissions , as given in Eq. 1. As it will be shown, the scenario-dependent carbon budget deviation strongly differs in magnitude, depending on which of the two cases we are looking at.~~ , where the direct mapping from cumulative emissions to temperature is of interest, not the 'remaining budgets'.

~~To see how the two above-mentioned interpretations of the carbon budget differ in regard to the scenario-dependent deviations they generate, we introduce two additional scenarios. The scenarios an follow identical mathematical structure as given in Eq. 4, except for a different boundary condition on emissions at t^*.~~

~~The first scenario (S1) is associated with the "net-zero" interpretation. In addition to boundary conditions given in Eq. 4, in S1 we require emissions to reach zero by the year t^* and stay zero from there onwards ($E(t \geq t^*) = 0$). Conversely, the second scenario (S2) associated with the "open budget" has no extra requirements on top of the ones given by Eq. 4.~~

The additional constraint on the emission pathway negatively affects the feasibility~~mentioned above~~. Therefore, ~~compared to S1 ("net-zero") , S2 ("open budget ")~~ the transient budget case has more possible emission pathway combinations available compared to net zero, which means ~~that a higher~~ a higher expected T_{d}~~is to be expected~~ .

3.1.3 Deviation ~~Time Evolution~~time evolution

~~Finally, the~~ The optimization procedure (Eq. (4)) calculates the extreme case of scenario-dependent deviations in one specific year t^* only. To see whether these deviations are persistent in time, ~~we design one extra experiment unique to S1. For each~~ an additional experiment is designed, one unique to the net-zero approach. For unit of k specified in the setup above, ~~we let the system~~ the system is left to evolve for the next 50 years following the optimization year ($t^* = 2070$), without adding new emissions~~and with it, allow~~ . Hence, $T_{\mathrm{d}}(k)$ is allowed to evolve freely in time, ~~whilst~~ while keeping cumulative emissions ~~on~~ at the same level. In ~~that way, we~~ this way, one can see how the scenario-dependent deviation obtained in t^* changes in time (again, independent of ZEC, as explained above).

3.1.4 Run ~~Configuration~~configuration

Preceding the initialization ~~in~~ of the optimization program, the ~~FAIR~~ FaIR model was historically forced from the preindustrial period (the year 1850) until ~~year~~ 2020 under the ~~same setup as for the Green's function generated, described in 2.2.2. The historical~~ RCP6.0 emission scenario. The quasi-historical run is dynamically separated from the optimization run since, in the former, emissions are prescribed, not generated by the program. The ~~meeting point is~~ two runs coincide in the year 2020, where the ~~historical run's variables' values~~ values of the historical run's variables are translated into the initial conditions of the variables of the full-fledged optimization run. Hence, $t_0 = 2020$ in Eq. (4) and the initial emissions value of the optimizer run ~~(E_0) are fixed to match the historical emissions in 2020.~~ equals to $E_0 = E_{\mathrm{RCP6.0}}(2020)$. The initial temperature at t_0 is ~~0.96~~ $T_0 = 0.96$ °C, with the associated ~~historical~~ cumulative emissions counting ~~584~~ $F_0 = 584$ GtC.

The Green's model ~~'s~~ run requires an additional modification to make it comparable with the ~~full-fledged~~ full model. As we can see in Eq. (2), Green's approach responds only to emissions ~~that we feed it~~ within the integral. That means that in the optimization run, which starts at t_0, it cannot capture the temperature response stemming from ~~the previous, historical emissions~~ emissions predating t_0. Conversely, this is not a problem for the ~~full-fledged modelsince that "leftover"~~ full model, since that 'leftover' temperature response is fed into the initial conditions of the run. To overcome this in Green's approach, we add the ~~"temperature leftover"~~'temperature leftover' parameter $T_{\mathrm{left}}(t)$ to Eq. (2), so it takes the form of $T(t^*) = \int_{t_0}^{t^*} E(\tau) f_{\mathrm{g}}(t^* - \tau)\mathrm{d}\tau + T_{\mathrm{left}}(t^*)$. The temperature leftover term is ~~easily generated using the full-fledged model , with the emissions following the historical run and then set to zero from 2020 onwards, where~~ generated by feeding the full model with RCP6.0 emissions until the year t_p, and then setting emissions to zero at the moment of pulse response generation. $T_{\mathrm{left}}(t)$ is ~~diagnosed~~ assessed as the temperature evolution ~~in the years when we stopped emitting.~~ after emission cessation. Various temperature leftover values corresponding to different t_p years are shown in Fig. 2. Note that the emission pathways and the years of emission cessation t_p correspond to those of pulse response generation (Fig. 1).

A final note to the reader in this regard: Unlike the net-zero case of scenario-dependent deviations (last subsection), the temperature leftover is de facto ZEC by definition – a temperature evolution following emission cessation.

3.2 Results

3.2.1 ~~"Net-zero Budget" (S1) Deviation~~

~~In the left panel of Fig. 1~~

3.2.1 Net-zero deviation

In Fig. 3, the generated ~~maximal (red) and minimal (light blue) temperatures for "~~deviations for the net-zero budget ~~" case are shown. The~~ case under one optimization setup are shown in light magenta. The chosen cap on cumulative emissions $F_{\mathrm{tot}} = 416$, in addition to the pre-2020 emitted CO_2, amounts to 1000 GtC, which approximately corresponds to the carbon budget allowed

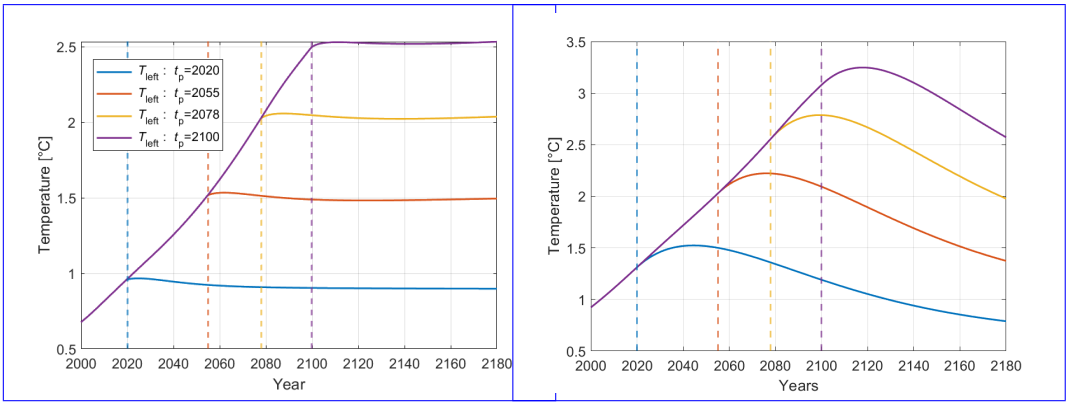

(a) Default parametrization FaIR (b) One-box model

Figure 2. Temperature evolution run up to (RCP6.0 emission scenario) and following the emission cessation at different years t_p. The blue line represents $T_{\text{left}}(t)$, added to Green's integral to compensate for the temperature evolution leftover from prior to the optimization year $t_0 = 2020$.

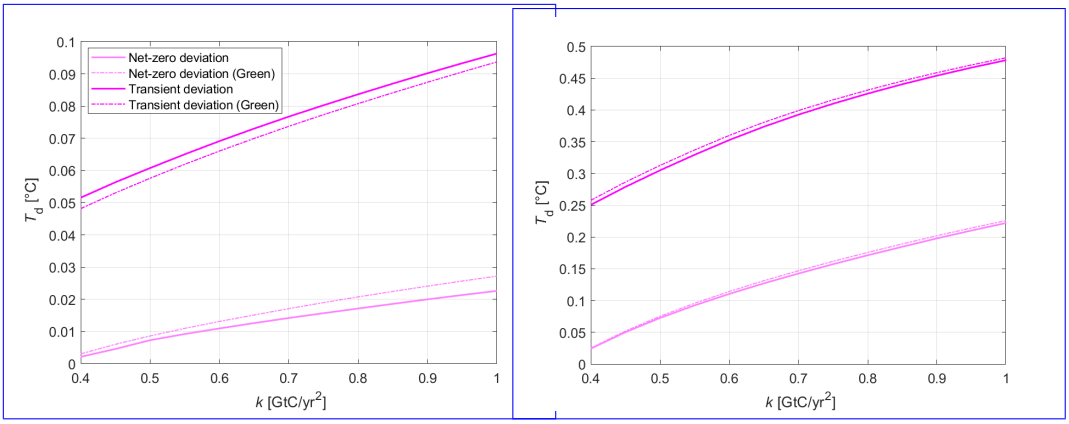

(a) Default parametrization FaIR (b) One-box model

Figure 3. Maximum scenario-dependent deviations, dependent on the maximum emission slope allowed k, generated by the optimization program described in Sect 3.1, with $F_{\text{tot}} = 416$ GtC and $t^* = 2070$. The solid and dashed lines represent the deviations generated by the complete models (FaIR on the left, one-box on the right) and their associated Green's function models.

for adhering to 2 °C with 67% probability, as suggested by the IPCC (Masson-Delmotte et al. (2021), Table SPM.2). The lower bound of $k = 0.4$ GtC/yr^2 is close to the feasibility limit, ~~detectable by the minimal and maximal temperature proximity. Furthermore, we can notice that both Green's (dashed line) and full-fledged (solid line) models follow a similar trend, with the former being shifted upwards due to the state-dependence of the carbon budget, discussed later. Finally, we can see that the maximal and minimal temperature (if focusing solely on a full-fledged approach) varies around 1.58~~ identifiable by the diminishing deviation. As expected, deviation increases with the k. The associated Min$[T(t^*)]$ and ~~1.59 °C, as opposed to the anticipated 2 °C following the IPCC suggested cumulative emissions amount. The difference is due excluding non-CO_2 forcers from our analysis and the parametrization choice~~ Max$[T(t^*)]$ from which the deviations are derived are shown in the figures in the Supplement. For demonstration purposes, the generated emission and temperature pathways for one choice of k are shown in Figs. 4c and 4d, which were generated by the FaIR and one-box model respectively.

~~The maximal scenario-dependent "~~In the case of FaIR, the magnitude of net-zero ~~budget" deviation T_d depending on the slope restriction k is plotted in the right panel in light pink as S1-FF for full-fledged and S1-G for Green's model , respectively. The deviation increases with the k. Furthermore, the deviation's magnitude~~ budget deviation is relatively small compared to the associated temperature increase. For the highest slope allowed ($k = 1\,\mathrm{GtC/yr^2}$), this setup's most significant possible deviation is approximately 0.025 °C, which amounts to roughly 1.5% of the overall temperature increase ~~. The upper bound of $T_d(k)$ is about 0.025~~ (roughly 1.58 °C, see Fig 4c).

Unlike FaIR, the one-box model shows far more pronounced net-zero carbon budget scenario dependency. In the case of one-box model in this setup, the deviation for the highest slope k is 0.225 °C ~~, accounting for only around one-quarter of a tenth of a temperature degree.~~ and hence amounts to roughly 10% of the overall one-box generated temperature increase (2.3 °C, see Fig 4d). As one can see, the one-box model generates about ten times larger deviations, compared to its FaIR counterpart.

~~Finally~~As for verification of Green's approach in the context of generating scenario dependency, the deviation derived from Green's ~~approach is in~~ function (dashed lines, Fig. 3) is the same order of magnitude as the deviation derived from ~~the full-fledged approach,~~ its associated full model (solid lines, Fig 3), and the trend behavior between the two is comparable. ~~This justifies using Green's function to explain the source of scenario-dependent deviations in Sect. 4.~~ The slight shift between the ~~full-fledged and Green'~~model's and Green's output is due to the fact that we use a constant Green~~'~~'s function, ~~and that effect will be even more pronounced with higher F_{tot} allowed~~ although the pulse response changes. This leads us to use the pulse response and its modification under different climatic conditions (Fig. ~~3) ; to be discussed in Sect~~1) to explain the source of scenario-dependent deviations in Sect. 4.

~~Figure 2 tests~~

3.2.2 Scenario-dependent deviation time evolution

Figs. 4a and 4b show the time persistency of detected $T_d(k)$. ~~Figure represents the time evolution~~ The figures represent the time evolutions of $T_d(k)$ (net-zero case) following the optimization year ~~t^*~~$t^* = 2070$, with different shades of red depicting the k range as given in the abscissae in ~~Fig. 1. The~~ Figs. 3a and 3b. Therefore, the initial values in the year 2070 correspond to the values of $T_d(k)$ ~~of the "net-zero" case (Fig. 1, right panel, S1-FF) . The~~ in Figs. 2 and 2b (light pink). Under the FaIR

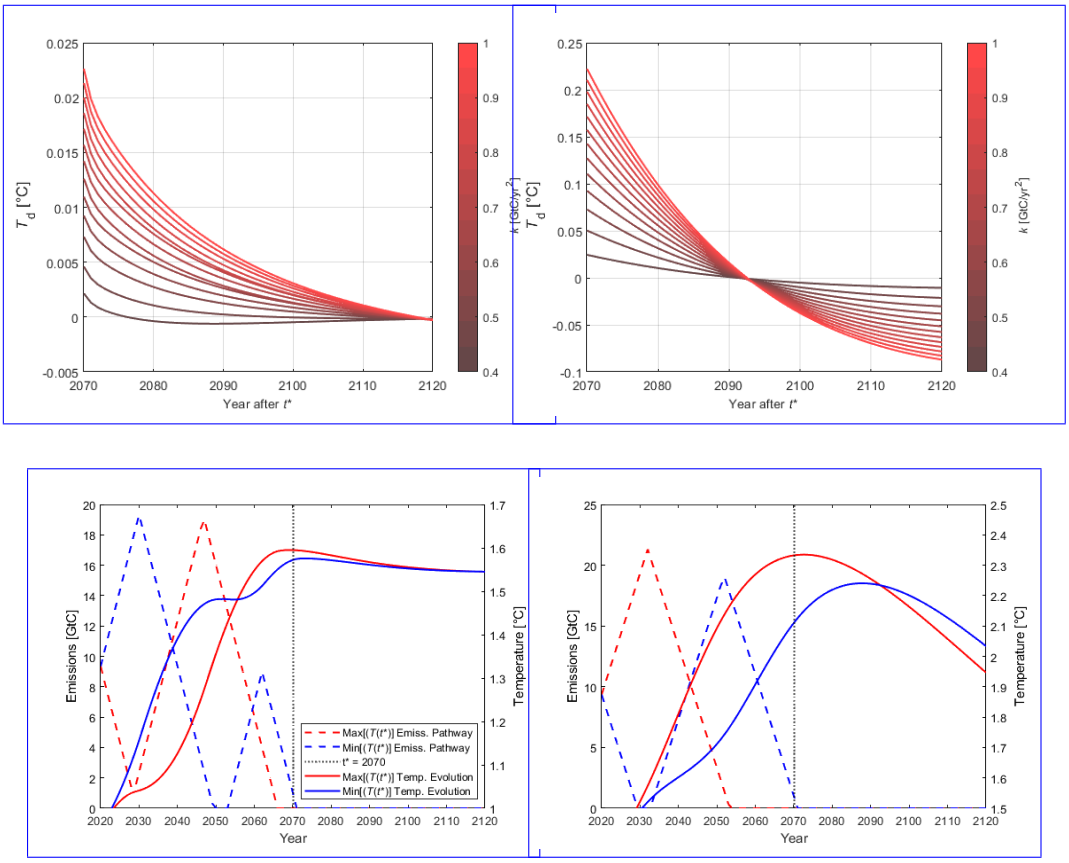

Figure 4. Graphs (a) and (b) show the temporal evolution of the net zero-case carbon budget deviation following the optimization year $t^* = 2070$, generated by FaIR and the one-box model respectively, under the setup discussed in 3.2.1. The colors represent deviations corresponding to the different k allowed, with the darkest red being the lowest allowed (0.4 GtC yr^{-2}) and the brightest red being the highest (1 GtC yr $^{-2}$). The generated emission pathways and absolute temperature evolutions corresponding to the optimization runs (both min. & max.) under the same setup for one value $k = 1$ GtC yr^{-2} are shown in graphs (c) and (d), generated by FaIR and one-box respectively.

model, the (already small) scenario-dependent deviation ~~, generated for $t^* = 2070$, dies out in time~~ ultimately disappears if no additional carbon ~~is added due~~ dioxide is added to the system~~coming to a dynamic equilibrium. This shows that the maximal~~ ; hence, the maximum deviations generated by the optimization program are only temporary~~and, in combination with their relatively small magnitude, one could safely ignore them.~~ . In contrast to FaIR, the one-box model's deviations do not 'die out' over time but decrease only to change sign.

~~The left panel shows the maximal and minimal temperatures depending on the maximal emission slope allowed (k), generated by the optimization program (Eq. (4)) with $F_{\text{tot}} = 416$ and $t^* = 2070$, while the right panel gives the associated scenario-dependent deviations given by subtracting Min(T^*) and Max(T^*). Different lines represent different run setups with a combination of abbreviations defining a specific run. The abbreviations used are S1 and S2 for the "net-zero budget" and "open budget" interpretations of the budget, and FF and G for full-fledged and Green's model, respectively. For example, *Max(T^*) in S1-G* represents the minimal generated temperature by Green's model for the "net-zero" case run.~~ The deviations' evolutions for $k = 1$ can be backtracked by examining the max. (red) and min. (blue) generated temperature evolutions shown in Figs. 4c and 4d, as the subtraction of the two yields the $T_{\text{d}}(k)$. The FaIR-generated min. and max. temperature pathways are divided at t^* but eventually coincide, just as the carbon budget approach suggests they should. In contrast, the one-box counterpart's temperature evolutions do not reach the same pathway within the time domain of interest.

~~Temporal evolution of the "net-zero" case scenario dependent carbon budget deviation, 50 years following the optimization year. The colors represent carbon budget deviation corresponding to different highest emission slopes allowed in the optimization process k, with the darkest red being the lowest allowed slope (0.4 GtC yr^{-1}) and the brightest red the highest allowed slope (1 GtC yr^{-1}).~~

3.2.3 Transient budget deviation

3.2.4 ~~"Open Budget" (S2) Deviation~~

~~In Fig. 1 are shown, the optimization run results for the "open budget", with the equivalent setup as for the "net-zero" (Subsect. 3.2.1) .~~

~~Focusing on the left panel, we see that the generated maximal temperatures (red) are the same for both cases. Furthermore, we can see that relaxing the condition on $E(t^*)$ leads to a significantly lower minimum temperature for the "open budget" (dark blue). The lower minimal temperature results from emissions allowed to stack up at~~ In Fig. 3 the transient budget deviations are shown in dark pink lines, under the optimization run with the equivalent setup as introduced in 3.2.1. Both for FaIR- and one-box generated deviations, the ~~end of the run (not being pushed towards zero as the "net-zero" condition requires).~~

~~Resultingly, there is a larger gap between the maximal and minimal generated temperature. Therefore, as shown on the right panel, the "open budget "~~ transient budget case shows a significantly larger scenario-dependent carbon budget deviation (dark pink) than ~~the~~ its net-zero counterpart (light pink). ~~For the~~ In the transient budget case, the FaIR-produced deviation is around 0.095 °C for the highest allowed k ~~. the deviation is around 0.095~~ only one-fifth that of the one-box model, which produces a maximum deviation of nearly half a degree (around 0.47 °C).

~~Left panels: Maximal (red) and minimal (blue) temperature dependent on k under the "open budget" case (S2), set up such that $t^* = 2090$ and $F_{\text{tot}} = (416, 600, 800, 1000)$ GtC. To get total cumulative emissions from preindustrial era, one needs to add 584 GtC to F_{tot} values, accounting for the emissions prior to t_0. The panels are ordered by the magnitude of the associated F_{tot}. Note that the y-axis domains are chosen to have the same relative interval of 0.3 °C but different absolute values. This way we shift the focus on the deviations and differences between Green's (G) and full-fledged (FF) model instead of the acquired absolute temperatures. Right panels: corresponding scenario dependent carbon budget deviation $T_d(k)$. Solid lines represent full-fledged, and dashed lines Green's approach.~~

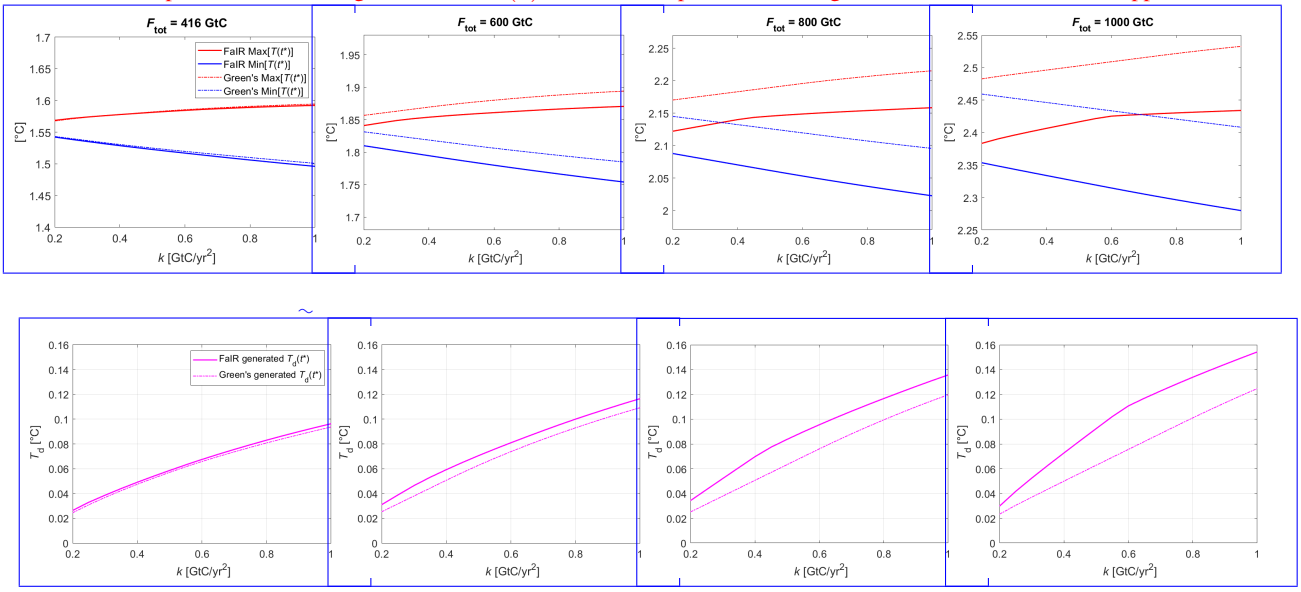

Figure 5. Top row: maximum (red) and minimum (blue) temperatures generated by the optimization program for the transient budget case, dependent on k, set up for different total cumulative emissions levels F_{tot} and $t^* = 2090$, with F_{tot} counted from the initial optimization year $t_0 = 2020$. The graphs are ordered by the magnitude of the associated F_{tot}. Y-axis domains all share the same relative interval of 0.3 °C, but different absolute values. Lower panels: corresponding scenario-dependent deviations T_d plotted against the respective k values. In all graphs, the solid lines represent the FaIR output; the dashed lines represent Green's output.

~~Finally, we can see that the feasibility limiting k is lower in the "open budget" than in the "net-zero" case – also a consequence of a~~ The difference is due to lower minimum generated temperatures, as a result of a non-constrained ~~$E(t^*)$.~~ ~~Hence, because the signal is much clearer~~ $E(t^*)$ and hence allowing emissions to 'stack up' toward the optimization year. This will become clearer in Sect. 4, where we discuss the effects of pulse response shape on the deviations.

The results presented in Figs. 3 and 4 are the last based on the one-box model prior to further analysis, since its simplicity does not allow us to see the effects of the changing climate (e.g. climate feedbacks) and hence the numbers demonstrate its underperformance. They are, however, also crucial to verifying the effects of the model's pulse response (Sect. 4). In the remainder of Sect. 3, the effects of different run setup choices on the FaIR-generated deviations are assessed.

Due to the feasibility issues, we opt for a ~~"open budget"~~ transient carbon budget approach to show how $T_\mathrm{d}(k)$ changes with the increasing total cumulative emissions F_tot. In Fig. ~~3~~5, the results of ~~four different optimization runs in the "open budget" approach are presented. The optimization year is~~ the optimizer in $t^* = 2090$ [3]~~, and cumulative emissions take the whole range introduced in the methods section~~for four different F_tot choices are presented, explicitly showing the generated min. and max. $T(t^*)$ dependent on k in the top row and and their corresponding $T_d(t^*)$ values in the bottom row. Three main effects can be ~~distinguished~~identified.

First, $T_\mathrm{d}(k)$ increases with higher cumulative emissions. A comparison of the ~~first and the last right panels~~ top to bottom graphs shows that the deviation ~~increased~~ increases by roughly 60%, ~~associated~~ in connection with the F_tot increase from 416 GtC to 1000 GtC. In the most extreme case with associated $F_\mathrm{tot} = 1000$ GtC, a deviation of ~0.15 °C is ~~detected~~produced.

Second, the choice of the optimization year t^* ~~seems not~~ does not seem to affect the deviation, if infeasibility effects are ignored. ~~Namely, one~~ One can argue that a difference between two examples in the lowest k choices can be ~~detected~~identified. This is where the infeasibility effect ~~occurs: the~~ manifests: The $t^* = 2090$ case has a slightly higher limiting k close to 0.1 GtC/yr^2. In comparison, the limiting k for $t^* = 2070$ is lower – visually depicted ~~with the meeting point~~ at the intersection of the corresponding blue and red lines on the left. The two are nearly identical from ~~from~~ roughly $k = 0.15$ GtC/yr^2 onwards. ~~Hence, one can conclude~~ In the supplement material, various combinations of the same cumulative emissions and different t^*'s show that the deviation ~~is not~~ not being a function of the optimization year is a robust result.

Third, ~~the gap between Green's model and its full-fledged~~ in the top row, the gap between FaIR and its Green counterpart's ~~maximal and minimal~~ maximum and minimum temperatures steadily increases with higher cumulative emissions F_tot ~~(left panels). This shift unambigously~~. Please note that the y-axis domains all share the same relative interval of 0.3 °C, but different absolute values. In this way, the focus is shifted to the changing difference between the Green's model-generated and FaIR-generated temperature with increasing F_tot.This increasing gap between the models' (Green's and FaIR) generated temperatures clearly indicates the inability of Green~~'~~'s model to capture non-linearities, as ~~discussed in the method section. Additionally, the $T_\mathrm{d}(k)$ difference~~ manifested by its use of the same, non-changing pulse response function as Green's function throughout the run. Furthermore, as shown in the bottom row, the difference in $T_\mathrm{d}(k)$ between the two models also increases with higher F_tot, albeit to a lesser extent. This effect can be attributed to the widening gap between the ~~maximal and minimal~~

[3] ~~The optimization year is pushed farther to increase the feasibility and signal clarity~~

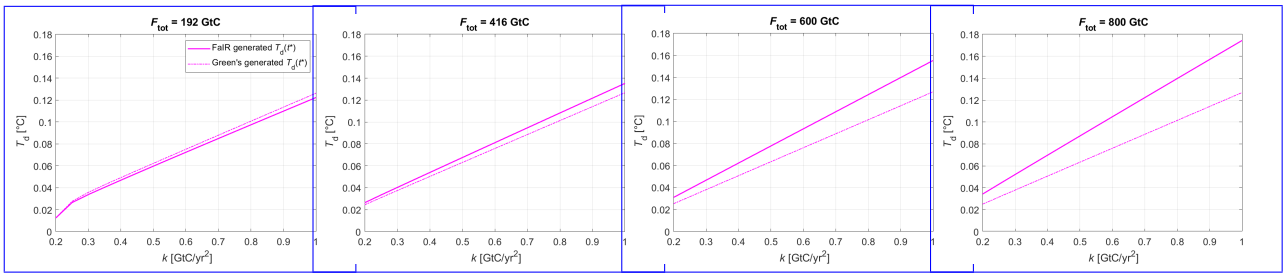

Figure 6. Scenario-dependent deviations, dependent on k, generated by the optimization program for the transient budget case with the allowed negative emissions, dependent on k, set up for different total cumulative emissions levels F_{tot} and $t^* = 2090$, with F_{tot} counted from the initial optimization year $t_0 = 2020$.

maximum and minimum temperature of the ~~full-fledged~~ FaIR approach, which increases its $T_{\text{d}}(k)$ to a larger extent ~~when compared to Green's model. As we show in~~ than does Green's model, due to the constancy of Green's function.

As shown in the next section, the last two findings can be interpreted through the lens of the pulse response function, ~~which changes in~~ the magnitude and shape of which change under different climatic conditions.

4 ~~Pulse Response as a Deviation Source~~

3.0.1 Effect of negative emissions

To round out this section, the effects of negative emissions on the transient budget's scenaro-dependent deviation are shown in Fig 6. The figure shows four different combinations of total allowed cumulative emissions F_{tot}, this time including a choice of $F_{\text{tot}} = 196$ GtC, which, when added to the cumulative pre-optimization emissions, reflects the carbon budget allowed for adhering to 1.5°C with 67% probability, as suggested by the IPCC (Masson-Delmotte et al. (2021), Table SPM.2).

As we can see in Fig. 6 (compared to Fig. 5), including negative emissions increases the generated T_d by roughly 0.04 °C compared to the zero negative emissions scenario, in the highest k case for all F_{tot} combinations.

4 Pulse response as a deviation indicator

In the previous section, ~~we have demonstrated~~ the extreme cases of scenario dependency ~~.irstly, we have shown that we can emulate the full-fledged model'~~were demonstrated. Firstly, it was shown that the SCM's generated scenario-dependent deviations can be emulated using a pulse response as Green's function (Eq. (2)). Hence, explaining the sources of scenario-dependent deviations by ~~inspecting~~ examining the pulse response~~'~~'s shape is justified. Secondly, ~~we have shown that~~ the gap between ~~full-fledged and Green's generated temperatures increases~~ the full model-generated and Green's model-generated temperatures is shown to increase with higher cumulative emissions. ~~As we will now show, this is because we use~~ This is

because a constant pulse response ~~in Green's approach, while in reality, the pulse also changes with higher~~ is used in Green's approach. At the same time, the pulse can change shape with changing climatic conditions.

In this section, ~~we contextualize~~ the carbon budget approach and its deviations are contextualized through the lens of the temperature response to an emission pulse. This ~~behaviour of the pulse response~~ pulse response behavior has broader implications ~~on~~ for other (simple) climate models and ~~to which extent~~ the extent to which they adhere to the carbon budget approach, with the one-box model serving as an example of inaccurate pulse representation and its consequences on deviation.

~~Temperature evolutions in response to 1 GtC emission pulse for different climatic conditions (colored) and the temperature response implied by Eq. (1) (black dashed). The numbers in the names indicate the global mean temperature anomaly under which they were generated. Green1 is a pulse response used as a Green's function (Eq. (2)) in the optimization runs (Sect. 3). Green1.5 corresponds to the pulse generated in the year 2055 of the RCP6.0 scenario run, with the corresponding cumulative emissions $F_{2055} = 959\,\mathrm{GtC}$, global mean temperature anomaly $T_{2055} = 1.5\,^{\circ}\mathrm{C}$, and a background atmospheric concentration $C_{2055} = 485\,\mathrm{ppm}$. Accordingly, Green2 is generated with the starting year 2078, $F_{2078} = 1317\,\mathrm{GtC}$, $T_{2078} = 2\,^{\circ}\mathrm{C}$, $C_{2078} = 577\,\mathrm{ppm}$, and Green2.5 with $F_{2100} = 1657\,\mathrm{GtC}$, $T_{2100} = 2.5\,^{\circ}\mathrm{C}$ and $C_{2100} = 660\,\mathrm{ppm}$.~~

4.1 Pulse ~~Response Shape~~ response shape as a ~~Scenario (In)Dependency Indicator~~scenario dependency indicator

To pinpoint the source of the deviations, ~~we first briefly revisit~~ a brief review of the discussion from Subsect. ~~2.2~~2.3 ~~. As~~ is called for. As previously shown, the ~~perfect~~ linear carbon budget (Eq. (1)) implies that the pulse response is a constant ~~step-function.~~ step function (Eq. (3), dashed black line in Fig. 1). However, the pulse response ~~function~~ functions used in Green~~'~~'s model, depicted in ~~Fig. 4 in blue, labelled as "Green1", shows a dynamical~~ blue and labelled pulse2020 in Fig. 1, show a dynamic temperature response.

Fig. 1, left graph shows the FaIR-generated Green's function (blue). In contrast to a constant step function, the initial response at the year of the emission pulse is zero. Then it ~~starkly~~ steeply increases until reaching a maximum value of approximately $1.7 \cdot 10^{-3}$ °C GtC^{-1}, 17 years following the pulse[3]. Furthermore, following the peak, there is a slow relaxation of the response, which slowly reaches a constant response later in time. Together, the non-instantaneous response followed by the sudden temperature increase and ~~the~~ temperature response peak ~~provides a hint for understanding the detected~~ can help to understand carbon budget scenario deviations in ~~Figures 1 and 3.~~ Figs. 3a and 5 (bottom row). In contrast, the relaxation following the temperature peak explains the ~~diminishing of the deviationlater in time~~subsequent diminishing of deviation, as shown in ~~Figure 2.~~ Fig. 4a. The relaxation of the temperature to a certain value is further confirmed by examining Fig. 4c: Even though two temperatures are generated, they eventually reach the same level, just as the pulse relaxation suggests they should. Namely, their cumulative emissions are equal, so their pulse response is the same.

To get ~~an intuition of~~ a better feel for the deviations and how they are connected to the pulse, ~~we~~ one can consider an extreme example. ~~Let us imagine~~ Say that all of the emissions are injected in one year. Total cumulative emissions will then amount to the value of the emissions injection only. Due to the pulse response, the temperature response will depend on ~~the time point~~

[3] ~~Note that using the FAIRv1.0.0 in Millar et al. (2017), the pulse peak is reached at year 12. The difference is because in the newer FAIR version the third temperature box was introduced, whilst previously there were only two. The slight shift of the maximum does not affect the brought up conclusions.~~

~~we are in . Following~~ what point in time we're at. Tracing the pulse response evolution, we ~~will detect a minimal~~ can see a minimum magnitude of temperature in the first year of the pulse and the ~~maximal~~ maximum temperature at the peak of the response, ∼17 years after the pulse. Effectively, ~~we have~~ these are two very different temperatures for the same cumulative emissions. The difference between ~~those two temperatures gives the maximally~~ the two temperatures is the maximum possible scenario-dependent carbon budget deviation. If the cumulative emissions then amount to 100 GtC, the pulse response scales accordingly, and the theoretical deviation ~~would be~~ between the minimum and maximum response is ~0.17 ~~°C between the minimal and maximal response~~ C. However, since ~~we introduced the slope restriction~~ in the optimization process, the slope restriction is fixed, and the initial emissions in 2020 ~~counted around~~ are set at roughly 10 GtC, the emission pathway is not nearly as steep, resulting in smaller ~~maximal~~ maximum deviations. In essence, the pulse response shows that if ~~we want~~ one wants to maximize the temperature response in a given year, ~~we~~ they should stack the emissions ∼17 years before that year; conversely, ~~if we want~~ to minimize the temperature response, ~~we~~ they should stack the emissions as close as possible (dictated by k) to that year.

Finally, because of the gradual relaxation of the response~~that comes in time, if we are~~ , if the year in question is far enough from ~~the time where~~ when we maximized the deviation, the deviation itself diminishes ~~–~~ – as shown in ~~Figure 2.~~ Fig. 4a. In the extreme case presented in the previous paragraph, ~~that~~ this can be intuitively seen as follows. ~~Albeit we could have~~ Although there could have been a considerable difference in temperature stemming from the same cumulative emissions between the 0th (the injection year) and 17th year (the peak year) following the pulse, ~~if we go further~~ going forward in time, the temperature response difference between the 80th and 63rd year following the pulse (~~likewise, 17 years~~ again, a 17-year difference) is ~~almost~~ virtually non-existent. Hence, the carbon budget deviation ~~"fixes"~~ 'fixes' itself as the system enters dynamic ~~equilibrium, which is an analogue of~~ relaxation, i.e., the pulse response ~~reaching~~ reaches a nearly constant value~~(relaxation)~~. Once it reaches the relaxation phase, the pulse response becomes very similar to the step-function response of the linear budget.

~~With this intuitive reasoning behind the (small)~~The Green's function used in Sect. 3 and derived from the one-box model is shown in Fig. 1b (blue). Unlike its FaIR counterpart, the one-box model's pulse response never reaches the relaxation phase and peaks much later (roughly 45 years after the pulse). As discussed above, it is these two properties that ensure low-level and non-persistent scenario-dependent ~~deviations, we deduct that the~~ deviation. Indeed, Sect. 3 shows that the one-box model produces much larger and persistent carbon budget deviations, which can then be directly attributed to its pulse response shape~~is~~ . The same arguments as for FaIR and its associated small deviations hold true for one-box and its associated larger deviations. For example, one can easily explain why the scenario dependency changes its sign (Fig. 4b) simply by looking at the pulse response of the one-box model. If we examine Fig. 1b, there is a considerable (positive) difference between the temperature at the 0th and the 45th (peak) year. By subtracting the peak temperature from the initial year's temperature, we arrive at a positive deviation. If we go farther forward, specifically 45 years, the observer who was in the initial year now sees their temperature response at the peak, while the observer who was in the peak temperature year now sees a much lower temperature. Subtracting the two now yields a negative value, even though the deviation was previously positive.

Hence, the pulse response shape dictates both the deviation and its evolution, making it critical for the climate model~~"~~'s adherence to the carbon budget approach. The ~~FAIR~~ FaIR model shows small, scenario-dependent deviations precisely because

its pulse reaches an almost constant regime relatively quickly following a peak. ~~If~~ Moreover, if a model cannot emulate reaching the temperature relaxation, it will also show much higher emission scenario-dependent deviations.

4.2 Pulse ~~Response Shape's Alteration~~ response alteration as a ~~State Dependency Indicator~~state-dependency indicator

Until now, ~~we have utilized (~~only a single pulse response (pulse2020) has been employed (Sect. 3) ~~and inspected (Sect. 4.1) a singular, non-changing pulse response.~~ as Green's function and examined in the previous subsection. However, the experiment shows that this pulse response ~~is not constant with the~~ changes with changing climatic conditions: ~~following~~ Following the same procedure described in ~~2.2~~2.3.2, ~~we generate pulse responses~~ pulse responses are generated later in the RCP emission run, accordingly. The generated pulses are depicted in different ~~colours~~ colors in Fig. ~~4.~~1 for both the FaIR and one-box models. The further analysis considers only the FaIR results, while one-box pulse alteration will be briefly commented on later, when the mechanisms behind the pulse alterations are discussed.

When comparing the pulses (Fig. 1a), a general trend can be ~~detected~~recognized. As the system ~~receives~~ is subjected to higher climatic stress in the form of higher cumulative emissions and higher temperatures, ~~the pulse response changes~~both the shape and the magnitude of the pulse response change. While all the pulse response variations show the aforementioned steep increase in the first few years following the pulse, the magnitude of the peak and the corresponding relaxation ~~response~~ temperature level decrease with changing climatic conditions.

This allows us to explain the ~~detected~~ widening gap between the ~~full-fledged and~~ FaIR-generated and corresponding Green's ~~model's generated maximal and minimal temperatures that increase~~ model-generated $\max T[(t^*)]$ and $\min T[(t^*)]$, which widens with higher F_{tot} ~~.~~ (Fig. 5, top row). Green's model ~~uses~~ (Eq. 2()) utilizes a non-state ~~dependent~~ -dependent (non-changing) pulse response as Green's function (~~Green1~~pulse2020). Therefore, it shows higher temperature anomalies for both ~~maximizer and minimizer~~ maximum and minimum compared with the ~~full-fledged~~ FaIR model, which by its ~~construction, is state dependent~~ nature is state-dependent in every sequential timestep (see ~~Appendix)~~Leach et al. (2021). The difference between the two models ~~gets more significant~~becomes more significant, the more stressed the climatic system is, as ~~shown in Fig. 3, left panels.~~ the pulse response used as Green's function moves farther away from the actual pulse response under the changed conditions.

~~Additionally,~~ In addition to the widening gap between the two models' generated ~~maximal and minimal temperatures, we have detected~~ min, and max. temperatures, the widening gap between the corresponding carbon budget deviations $T_{\text{d}}(k)$ is identified. Fig. ~~As we can detect in Fig. 3, right panels, the gap increases in favour of the~~ 5 (bottom row) shows the increasing gap between them, in favor of the FaIR model's lower ~~full-fledged model's~~ acquired T_{d}. This can be explained by the flattening of the pulse response curve with higher climatic stress. Green~~'~~'s approach utilizes ~~the Green1~~ pulse2020 as a pulse response, which has a distinctly ~~higher "peak belly"~~ larger 'peak belly' than its counterparts. ~~Conversely, the full-fledged model incorporates feedback, and its response acts accordingly, as these two effects show.~~

One could have also opted for a different Green~~'~~'s function that would reduce the aforementioned gaps between ~~the full-fledged and Green'~~FaIR and Green's model, but then the choice ~~is case specific. Green's model would~~ would be case-specific.

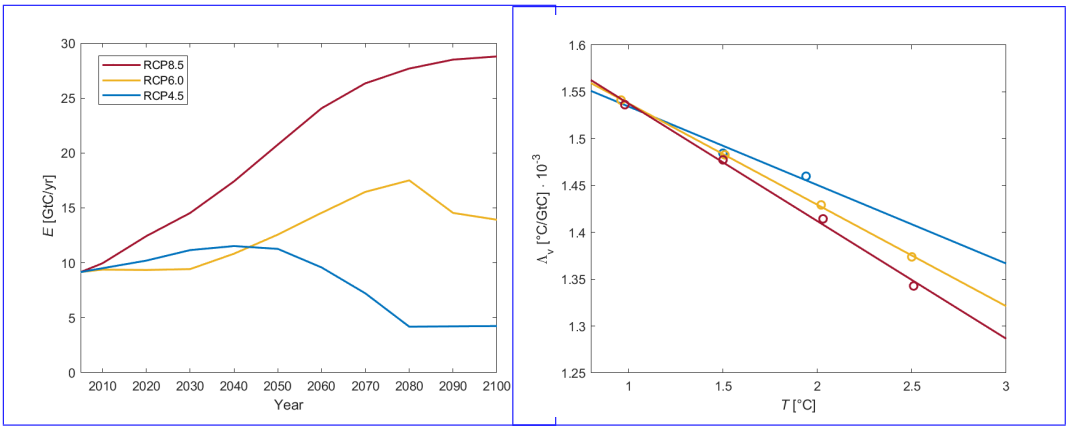

Figure 7. Right graph: TCRE approximations $\Lambda_v(T)$ generated from pulse response functions under different climatic conditions and emission scenarios. Scatter plots are actual values of Λ, while the line is the result of linear regression. The different colors represent the Λ_v dependencies generated from different RCPs, which are plotted in the left graph.

Green's model could be more precise depending on ~~if~~ whether or not we generated Green~~'~~'s function closer to the climatic conditions we ~~want to inspect~~were interested in. Hence, Green~~'s Approach~~ 's model can indeed be seen as a linearized and simplified full model, as the theory suggests. Hypothetically, if the change ~~of the pulse response f_g~~ in pulse response f_g with climatic conditions could be incorporated into Eq. (2), the gap between the two approaches would decrease ~~– if not become non-existent~~ if not disappear entirely.

5 ~~State-Dependent Deviation~~

4.1 Changing pulse response as a variable TCRE: nonlinearity of the carbon budget

As discussed in the introduction, the previous literature ~~has suggested~~ suggests that TCRE is not a constant value but slowly decreases with cumulative emissions. This can be interpreted as the carbon budget~~(climate~~'s (=climate's) state dependence~~.~~ ~~While it was previously numerically detected, here we offer a way to quantify it explicitly in the form of a new, state-dependent~~ , which manifests in the non-linear carbon budget equation ~~. The changing temperature response pulse is crucial in deriving the new equation.~~ (Nicholls et al., 2020). This non-linearity can be identified by the change in pulse response shape with changing background climate conditions.

4.1.1 State-dependent pulse response as a variable TCRE

4.2 ~~State-Dependent Pulse Response Approximation: a State-Dependent TCRE~~

In Subsect. ~~2.2~~2.3.3, it was ~~already~~ shown how the ~~"perfect budget"~~ step-function pulse response in Green~~'~~'s model translates into ~~the~~ TCRE included in Eq. (1). If the TCRE ~~decreases~~ changes with background conditions, the ~~"perfect" step pulse should also decrease~~ linear carbon budget step-function pulse (black dashed line, Fig. 1) should also change in magnitude following the climatic stress. Indeed, ~~we showed how that actual~~ Fig. 1 shows that the SCM-generated pulse response decreases in magnitude with background conditions. If ~~we approximate it with a~~ then the changing pulse is approximated with a changing step function, the decrease of the pulse response can be directly linked ~~with~~ to the decrease of TCRE. ~~Keep in mind, however, that with that approximation, we lose~~ With that approximation, however, the ability to express the time delay and scenario dependency ~~;~~ is lost, as the shape of the pulse response function dictates the scenario dependency ~~.~~ (Sect. 4.1). As they were shown to be small, this aspect can be safely ignored. Motivated by the findings in ~~Subsect~~Sect. 4.2, ~~we attempt~~ in this subsection, a method for using a pulse response representation to explicitly quantify ~~the~~ TCRE dependency on climatic conditions ~~in this subsection. The method employed is~~ is developed, as follows.

To generalize the analysis, ~~we generate pulses~~ the additional pulses are generated under RCP4.5 and RCP8.5 emission scenarios, ~~in addition to~~ along with the already generated pulse responses under different climatic conditions with RCP6 ~~. We mimic the procedure from the last subsection and the method section, generating the first pulse~~ (Fig. 1). The first pulse of each run is generated at the benchmark year ~~of~~ 2020 and the rest at the same temperature levels ~~, where possible. For RCP6, the climatic conditions under which the comparison pulses were generated are listed in Fig. 4 caption. Using RCP4.5 scenario, pulses are generated in years $t_{RCP45} = (2020, 2051, 2100)$ yr and the corresponding climatic conditions $F_{RCP45} = (588, 944, 1259)$ GtC, $T_{RCP45} = (0.96, 1.5, 1.94)$~~ (1.5, 2 & 2.5 °C~~and $C_{RCP45} = (404, 482, 529)$ ppm. For RCP8.5, the values are $t_{RCP85} = (2020, 2043, 2061, 2075)$yr, $F_{RCP85} = (614, 966, 1354, 1716)$ GtC and $T_{RCP85} = (0.98, 1.5, 2.03, 2.51)$ °C~~), where possible.

Next, recalling the ~~"perfect budget " discussion, we approximate~~ perfect budget discussion, the generated pulses are to be approximated with the step function. Ignoring the temperature evolution dynamics in the early years of the pulse response, the pulse is ~~approximated with a constant Λ~~ transformed into a constant Λ_v by averaging it between years 70 and 80[3]. As shown in Fig. ~~4~~1, the pulse dynamics ~~relaxed~~ relax by that time, reaching ~~a~~ relative constancy. ~~Using this approximation, we ignore the temperature response dynamics. We justify this choice by the fact that extreme scenario-dependent deviations generated are relatively small and only temporary. In the long term, the constancy of the pulse dominates the behaviour.~~ After approximating the pulses, ~~to each value of generated Λ we assigne its~~ , the corresponding cumulative emissions and temperature values (~~e.g.~~i.e., the background climatic conditions under which the original pulse was generated) ~~. With that, we have a mapped $\Lambda(T, F)$ dependency~~ are assigned to each value of generated Λ_v. By doing so, the $\Lambda_v(T, F)$ dependency is mapped, which,

[3] In ~~that~~ this way, the approximation for each pulse resembles the black dashed line in relationship to the blue line in Fig. ~~4~~1.

which when reasoned in line with Eq. (1)[4], can be considered a TCRE dependent on cumulative emissions and temperature increase.

With the first effectIn this way, the carbon budget's state dependency is made explicit. Looking at : Examining each RCP case separately , we can infer that Λ decreases linearly both shows that Λ_v decreases linearly in T and F . under the standard FaIR parametrization (Fig. 7b). Moreover, looking at the right figure, we one can see that by adding 1000 GtC, $\Lambda(F)$ dropped $\Lambda_v(F)$ drops by roughly 10%, which is in accordance keeping with the findings from of Leach et al. (2021).

Secondly, the linear relationship between Λ and T and F seems to change depending on the RCP scenario in which it was generated. We can see that the (negative) slope of $\Lambda(T)$ and $\Lambda(F)$ increases as the emission scenario becomes more emission intense. In absolute terms, it is lowest for RCP4.5 and highest for RCP8.5. This finding indicates that there could be another layer of carbon budget deviation, which could be seen as a "scenario-dependent state dependency". We take that finding with a grain of salt since it comes about following several approximations – investigating the underlying reasons is left for future research.

4.1.1 From pulse response to carbon budget equation

4.2 State Dependent Carbon Budget Equation

If we focus only on one RCP runs' generated Λ's, we can analytically derive the carbon budget state dependency The RCP6-generated Λ_v (Fig. 7b, yellow dots) is chosen to derive the carbon budget's state dependency from the pulse response representation. The choice of RCP scenario does not constrain the conclusions of this exercise. Fig. 7b suggests a linear relationship $\Lambda_v(T) = -\mathrm{a} \cdot T + \mathrm{b}$, with $\mathrm{a} = 1.083 \cdot 10^{-4}$ GtC^{-1} and $\mathrm{b} = 1.646 \cdot 10^{-3}$ °C GtC^{-1} derived via linear regression. Therefore, TCRE (here Λ_v) is reinterpreted through the lens of T dependency, as temperature is a thermodynamic variable driving the system change. This way, assuming any function for the state dependency is avoided; rather, it is deducted from mapping $\Lambda_v(T)$ (Fig. 7, right graph). For RCP6 scenario, we acquire a and b by linear approximation of the point values $\Lambda(T)$, which gives $a = 1.083 \cdot 10^{-4}$ GtC^{-1} and $b = 1.646 \cdot 10^{-3}$ °C GtC^{-1}, so that $\Lambda(T) = -\mathrm{a} \cdot T + \mathrm{b}$.

Since Λ Λ_v is, by definition, a temperature response to an emission pulse, we interpret the temperature change following the approximated pulse is interpreted as $\Delta T = \Lambda(T) \cdot E_{pulse}$. In other words, the temperature change is equal to one unit of pulse emission scaled by temperature response to a pulse Λ. Using Λ_v. Given the fact that the emission pulse brings about the a change in cumulative emissionswe rewrite the forementioned relation in the form of a differential equation, the aforementioned relation is rewritten in differential form as:

$$\mathrm{d}T = (-\mathrm{a} \cdot T + \mathrm{b})\mathrm{d}F. \tag{5}$$

[4]Note that Λ and λ Λ_v have the same function in the "perfect budget" equation. The difference is that λ Λ is a constant, while Λ Λ_v is a function of temperature and cumulative emissions.

~~TCRE approximations A generated from pulse response functions under different climatic conditions and emissions scenarios. The middle panel shows A's dependency on cumulative emissions, and the right panel on global mean temperature anomaly. Scatter plots are actual values of A, while lines are corresponding linear extrapolations. Different colours represent A dependencies generated from different RCP scenarios that are plotted in the left panel.~~

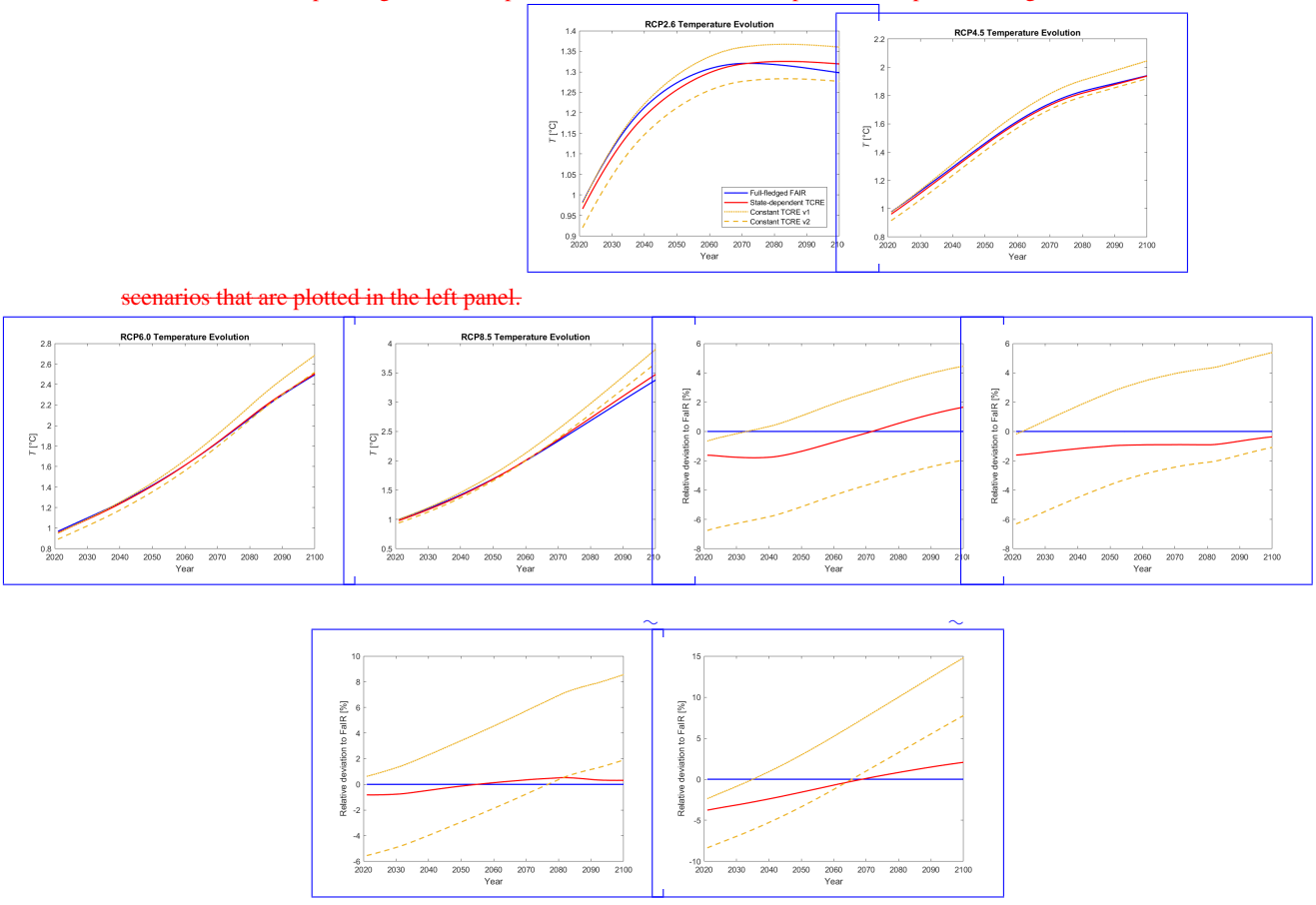

Figure 8. Top row: Temperature evolution under the three RCP emission scenarios, calculated by the full-fledged FaIR model (blue), the derived non-linear carbon budget equation (Eq. (6) (red), and the linear carbon budget equation (Eq. (1) with two different TCRE values (yellow)). Bottom row: Corresponding relative deviations of generated temperatures from FaIR-generated temperature, in percentages.

Solving this ~~form of~~ differential equation analytically is fairly straightforward. Hence, ~~integrate~~ by integrating Eq. (5), ~~and we get:~~ one arrives at:

$$T(F) = \frac{b}{a}\frac{\mathrm{b}}{\mathrm{a}} + (T_0 - \frac{b}{a}\frac{\mathrm{b}}{\mathrm{a}})e\mathrm{e}^{-a(F-F_0)}, \tag{6}$$

~~In its essence~~with T_0 and F_0 being the initial values at the time of the first pulse (pulse2020). Essentially, Eq. (6) represents ~~an improved, state-dependent version of the~~ a non-linear carbon budget equation ~~. Instead of linear, it has a weakly negative exponential temperature dependence on cumulative emissions~~under a default FaIR parametrization.

~~To get information about its shape in the relevant domain, we insert the values of the constants. Since we generated pulse responses only from 2020 onwards, we chose that year for our initial conditions~~[5]~~, so $T_0 = 0.955$ °C and $F_0 = 584$ GtC. The values of a and b are listed in a few paragraphs above. Numerically, we get $T(F) = 15.1985 - 14.2434e^{-0.0001083(F-583.58)}$.~~ ~~If~~ When plotted, one can see that $T(F)$ is a closely linear, slightly concave function within the F domain of interest[5]. ~~What is important is that the ratio between temperature and cumulative emissions changes with changing cumulative emissions, and hence, it captures state dependency.~~

~~As a side note, one could ask why we derive the equation with A mapped with temperature instead of cumulative emissions, as both pieces of informations are available in Fig. 5. The main argument is that we deem temperature to have more physical meaning than cumulative emissions when it comes to the natural system. Nevertheless, we could easily redo the derivation with a mapped $A(F)$ and get another form of state-dependent carbon budget equation where the temperature is a quadratic function of cumulative emissions. If a user finds quadratic form more useful~~[6]~~, it is not a problem since the two equations give the same temperature diagnoses, at least in the tests done for Eq. 6.~~

To check if ~~the newly introduced~~ Eq. (6) ~~is reasonable in that it generates~~ yields correct temperature dynamics, ~~we test it with RCP emission scenariosplotted in Fig. 5, left panel. We plot the generated temperature evolutions in Fig~~it is tested against the full FaIR model under the aforementioned RCP scenarios. ~~6 (redlines~~The resulting temperature pathways are plotted in the top row of Fig. 8 (red) alongside the ~~full-fledged FAIR~~ FaIR output (blue~~lines~~) and the linear carbon budget Eq. (1) with two values of constant TCRE (yellow~~lines)for each RCP scenario. Firstly, however, we scrutinize the implication of choosing a constant TCRE.~~

~~To understand how the choice of constant TCRE affects the temperature evolutions, we use~~), while the bottom row shows the corresponding relative deviations from the FaIR-generated temperature pathway. The two TCRE values ~~: the higher one,~~ are TCRE_{v1}=$1.6 \cdot 10^{-6}$ °C GtC^{-1}, and ~~the lower~~ TCRE_{v1}=$1.53 \cdot 10^{-6}$ °C GtC^{-1}~~, the latter being given as a mean TCRE value in Leach et al. (2021) . As we can see in the figure, the higher choice of constant TCRE results in an~~ .

Choosing a larger constant TCRE (v1) results in a more accurate temperature diagnosis in the first half of the century ~~. However, it overestimates the temperature in later years (higher cumulative emissions) compared to full-fledged FAIR~~under

[5] ~~These are the same initial conditions as for the full-fledged approach in the optimization run.~~

[5] Note that ~~F~~ here F represents the total cumulative emissions from the preindustrial era. One could rewrite the equation with $\Delta F = F - F_0$ to ~~get~~ derive the temperature increase relative to the initial year ~~, here chosen to be 2020.~~$t_0 = 2020$.

[6] ~~The quadratic form reads as: $T(F) = \frac{a'F^2}{2} + b'F + (T_0 - \frac{a'F_0^2}{2} - b' \cdot F_0)$~~

lower cumulative emissions, with deviations increasing in step with rising emissions. The opposite is true for ~~the lower choice of TCRE, and we can discern that in Leach et al. , TCRE was gauged to fit higher climatic conditions. In that~~ a smaller TCRE. In this sense, Eq. (1) with a constant TCRE is a linearized version of ~~FAIR~~ FaIR in a similar way as ~~Green'~~ the Green's function model but without the ability to generate ~~scenario dependent~~ scenario-dependent effects. Additionally, we can ~~detect~~ see that the state-dependent deviations are not transient ~~as~~ like their scenario-dependent counterparts, but ever-increasing with the changing cumulative emissions. The highest detected absolute deviation is around ~ 0.5 °C for the end-of-the-century temperatures in the RCP8.5 run, which amounts to $\sim 15\%$ relative deviation from the FaIR-generated temperature.

Unlike constant TCRE, ~~our newly introduced state-dependent carbon budget~~ Eq. (6) replicates ~~full-fledged~~ the FaIR generated temperatures in RCP2.6, RCP4.5, and RCP6 runs ~~almost perfectly. A drift is detectable for higher temperatures in the RCP8.5 and can be attributed to the Λ having a steeper linear decrease with F and T (Fig. 5) under the RCP8.5 scenario than~~ relatively well, with the ~~RCP6 one, the latter being chosen to generate Eq. (6). The maximal~~ relative deviation from FaIR being less than $\sim 2\%$ throughout the century. The largest absolute drift from the ~~full-fledged model's generated~~ FaIR-generated temperature is around 0.1 °C at the end of the century ~~.~~ under the RCP8.5 scenario. However, this degree of drift is less than 3% in relative terms. Since RCP8.5 is arguably somewhere in the upper ~~boundary~~ bound for possible emission pathways ~~, we can safely say~~ (and RCP2.6 arguably a very optimistic lower bound scenario), one can conclude that Eq. (6) is a good emulator of ~~the full-fledged FAIR model and a state-dependent enhanced carbon budget equation, at least for the standard parametrizationused throughout the paper~~FaIR under the single, default parametrization. The incorporation of climate parameters in Eq. (6) ~~, and its scrutinization~~ and assessing it in view of climate economics ~~will follow this work~~lie beyond the scope of this paper.

4.2 Uncertainty in pulse response

By considering the pulse response representation and its implications on the carbon budget framework under one FaIR parametrization, the effects of different model calibrations on pulse response and, thereby the carbon budget are evaluated in the final part of this paper.

Fig. 9 shows pulse responses generated as described in 2.3.2 under six different sets of FaIR parameters, each tuned to a different CMIP6 model, with Fig. 9e being the default parametrization used in the rest of the analyses. We can see that every calibration yields a distinct pattern of behavior. Using the framework from the rest of Sect. 4, one can deduct how each calibration affects FaIR's adherence to the carbon budget approach

To examine scenario dependency, one must examine pulse response shape (Sect. 4.1). Looking at Fig. 9, we can see that all of the parametrizations show a relatively small scenario dependency, as all of them show pulse responses that peak in 10-20 years, followed by some degree of relaxation in the time domain of interest. In other words, one can imagine approximating them with a step function. Two parametrizations that stand out are MIROC-ES2L and ACCESS-ESM1-5. The former reaches a peak and then continually decreases, although at a much slower rate than the one-box model (Fig. 1b). Hence, the scenario-dependent deviations will not fully diminish and are likely to change sign, as per the discussion associated with 3.2.2 and Fig. 4. The

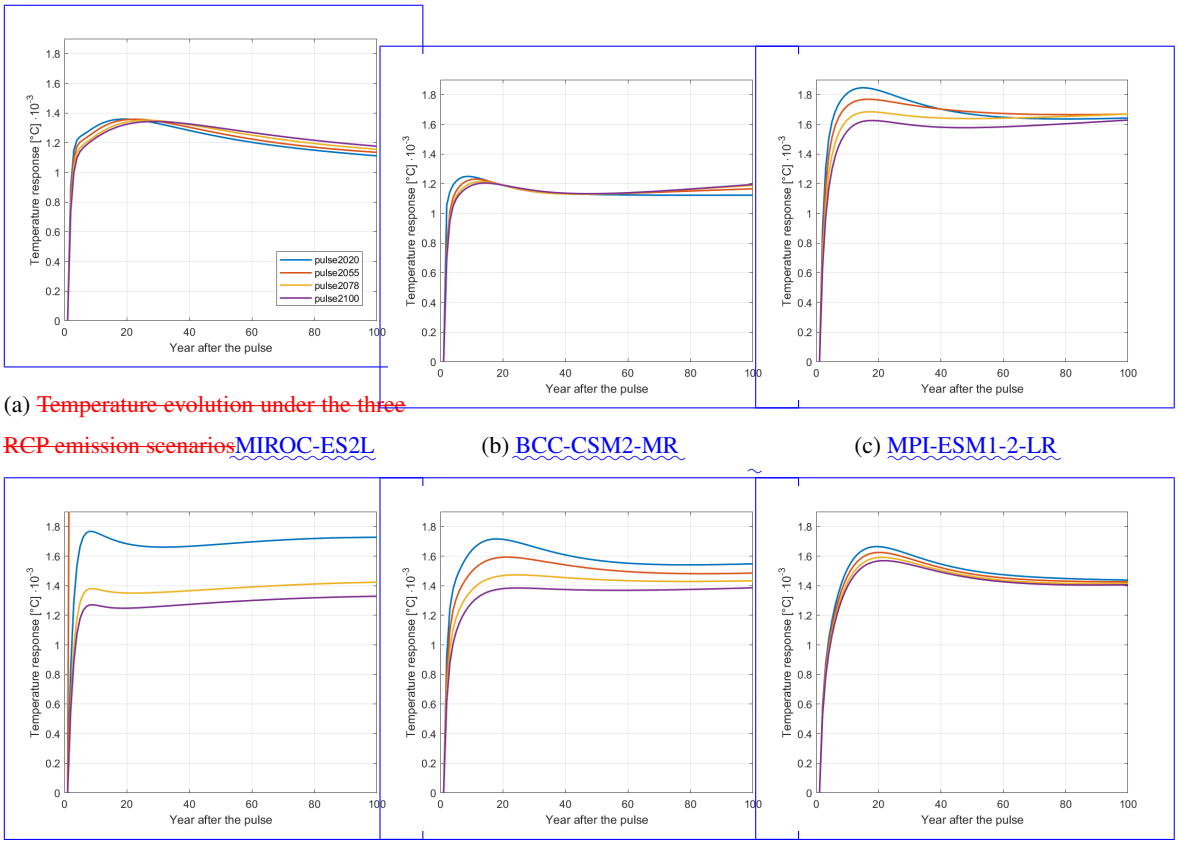

(a) ~~Temperature evolution under the three RCP emission scenarios~~MIROC-ES2L (b) BCC-CSM2-MR (c) MPI-ESM1-2-LR

(d) ACCESS-ESM1-5 (e) Default (f) CNRM-ESM2-1

Figure 9. Pulse responses under different FaIR calibrations. Different parameter sets are each tuned to a specific ESM, with parameter values given in Tables 2 and 3 in Leach et al. (2021). Note that graph (e) matches the left graph in Fig. 1, included here for comparison.

same holds true for the latter, although in the other direction as the pulse response of ACCESS-ESM1-5, as the temperature gradually increases following the pulse.

In the context of state-dependent deviations, ~~as calculated by the full-fledged FAIR model (blue), the newly introduced state-dependent carbon budget equation (Eq. (~~Fig. 9 reveals an interesting effect of different FaIR parametrizations on the non-linearity type of carbon budget equation. In Sect. 4.3, it was shown that the changing TCRE under different climatic conditions can be reinterpreted as the changing pulse response through $\Lambda_v(T)$. Additionally, it was shown that a decreasing $\Lambda_v(T)$ (Fig 7, right) leads to a concave non-linear carbon budget equation (Eqs. (5) and (6~~)) (red), and the "perfect budget" equation (Eq. (1)) with two different TCRE values (yellow). The state-dependent~~)). The opposite also holds true: If $\Lambda_v(T)$, and hence the pulse response increases in magnitude with higher temperatures, it results in a convex non-linear carbon budget equation. Ultimately, if the pulse response magnitude does not change with changing background conditions, the carbon budget

equation ~~is a very good emulation of the full-fledged model. In contrast, the constant~~ is indeed linear[6]. With that in mind, one can easily deduct that not all the combinations of FaIR parameters lead to the concave carbon budget equation~~can emulate the full model in a specific domain only, depending on how it is calibrated; e.g. for a higher TCRE chosen value~~ , as derived in Eq. (~~v1), Eq~~6). For example, MIROC-ES2L tuned to FaIR indicates a slightly convex budget equation, while BCC-CSM2-MR and CNRM-ESM2-1 are closest to the linear carbon budget. ~~1 is a good fit in the early years of the RCP runs but starts to drift away from the full-fledged model with higher temperatures.~~

5 ~~Discussion~~

~~In this paper, we focused on the deviations from the carbon budget, formalizing a distinction between the carbon budget emission scenario-dependent and climate state-dependent deviation, both logically independent. By state-dependent deviation, we mean the change of TCRE value, depending on the background climatic conditions – specifically, the cumulative emissions and global mean temperature increase. By scenario-dependent deviation, we mean the possible difference in temperature that comes solely from the preceding emission choice while keeping cumulative emissions fixed. We explicitly calculated the maximal possible scenario-dependent carbon budget deviations. Furthermore, we offered a reinterpretation of~~ This will be explored further in future work. Due to the constrained set of fully accessible different parameter sets, only six calibrations are presented here. A larger set would provide some insights into which elements of FaIR drive which types of behavior. Additionally, it would be interesting to see to which extent FaIR tuned to a CMIP6 model reproduces the behavior of its corresponding ESM under the same setup. If it were found to do so, one could extend the pulse response framework with FaIR tuned to ESMs to analyze carbon budget deviations as given by the ESM.

5 Discussion

The work shown here utilizes FaIR, the one-box model, and the associated Green's function models. The non-linearities appear in FaIR in both the carbon cycle feedback and in the temperature response saturation. As pointed out in the introduction, the interplay between the changing carbon cycle and temperature response produces the near-linearity of the carbon budget equation, with the former being a convex and the latter a concave driver of the budget equation. equation.

The second model used in the analysis is the ~~carbon budget approach through the lens of Green's function formalism, encapsulating the scenario dependency. We connected the change of pulse response under climatic change and derived a new carbon budget equation; henceforth, we derived a new analytical form of~~ one-box model, introduced as an example of a model with a dramatically different pulse response than FaIR, which facilitates comparison in the context of the pulse response behaviour effect on the carbon budget approach deviations. In contrast to FaIR, the ~~carbon budget equation that captures state dependency. This last section summarises the findings and emphasises their broader implications~~one-box model does not include climate feedbacks on the carbon cycle, so non-linearities arise only through the saturation in temperature response.

[6] Note that a pulse relaxation is still a necessary requirement.

Section 2 introduced the FAIR model, a simple climate model with four carbon and three temperature compartments. The FAIR model is chosen for the analysis for several reasons: firstly, it has the ability to capture climate feedback on the carbon cycle; secondly, The inclusion (or lack) of climate feedbacks has an effect on how the pulse response changes with changing climatic conditions. In the one-box model, the carbon cycle response stays the same regardless of background conditions, so the model has already been praised in the literature for its efficiency; thirdly, it is relatively easy to implement and is computationally cheap; lastly, and most importantly for this paper, it can correctly capture the temperature response to emission pulse (e.g., pulse response). As we show in the paper and deem it the central finding, the pulse response behaviour reveals the climate model's degree of both scenario and state-dependent carbon budget deviationsis modified only by logarithmic temperature response saturation. This manifests in the pulse changing magnitude but not shape (Fig. 1b). Conversely, including climate feedbacks changes the shape of the response function and modifies its magnitude. For a more detailed discussion on how the climate feedback changes the carbon cycle in FaIR in the context of decreased atmospheric CO_2 decay, see Millar et al. (2017).

To test whether pulse response behaviour is trustworthy to give us information on behavior offers a trustworthy framework for explaining carbon budget deviations, we incorporated it in it is employed as a Green's function in Eq. (2). The methodology is explained in detail in the introduction. However, by proposing Eq. (2) and using a FaIR-generated (or one-box-generated) Green's function, we assume that the form of Green's function. We have shown that if the relationship between temperature increase and cumulative emissions is purely linear without any time delay, the pulse response ought to be a constant step function, independent of background climate conditions. Plugging in the step function as a Green's function indeed leads to the "perfect carbon budget" equation which gives the first proof of Green's concept under the umbrella of the carbon budget approach. climate model is a set of linear differential equations. Hence, although Green's model has been proven to capture scenario-dependent effects, the effects of climate change on the carbon budget approach cannot be explicitly captured with Eq. (2). This effect is visible when comparing the full model and Green's model optimization runs, as the two sets of generated temperatures have an ever-increasing gap with higher cumulative emissions (Fig. 5, top row). One could modify Eq. (2) so as to include a changing pulse response instead of a fixed f_a, but this remains theoretical; the implementation is unclear.

Regardless of Green's model's inability to correctly forecast (or hindcast, for the same reasons) temperature evolution, Sect. 3 shows that it is indeed capable of mimicking the scenario-dependent deviations of both FaIR and the one-box model. Even though there is an ever-increasing gap between temperatures generated by the full model and Green's model, the scenario-dependent deviations are well represented by Green's function even for higher F_{tot}. Hence, one concludes that state and scenario dependencies can arise independently.

In Sect. 3, we compare the pulse response (Green's) concept with the full-fledged essence, the results show that the changing of the pulse under changing background conditions does not affect Green's model's ability to predict scenario dependency. This implies that one could use any model, of any complexity, generate its pulse response and then plug it into Green's model under the optimization procedure that maximizes/minimizes the temperature in a run under fixed cumulative emissions. In this experiment, we effectively test both the extreme cases of program (Eq. (4)) to arrive at the corresponding model's possible scenario-dependent deviations (focusing on strictly FAIR model results)and numerically test whether the introduced Green's

approach can replicate the full-fledged modeldeviations. In the case of a complex climate model (e.g. an ESM), this would be possible only through the Green's function approach due to the unacceptable computational time [7] required to run an ESM in an optimizing program.

When quantifying the it comes to purely numerical findings in the context of scenario-dependent deviations, it was shown that how much we emit after the optimization year would drastically can dramatically affect the generated deviations; we differ two cases: the "net-zero" and the "open budget" interpretation. In the former, no emissions are allowed after the optimization year t^*, de facto reaching and staying at net-zero after t^*; in the latter, that condition is non-existent. The highest . For FaIR, the largest possible deviation we acquire is approximately 0.15 °C for the "open budget " transient budget case. In the net-zero case, the highest deviation is way largest deviation is well below 0.1 °C. From the policy-relevant carbon budget viewpoint, this is good news, as it keeps the carbon budget approach resistant to scenario choice when while complying with specific temperature targets and net-zero commitments. Regardless of the interpretation, the carbon budget scenario-dependent deviations we detected identified are not permanent but a result of the optimization in one a specific year. The arguably small deviation subsides diminishes relatively quickly if we allow the systemto go towards dynamic equilibriumno further emissions are added to the system. Furthermore, we showed that scenario-dependent deviations increase with the higher cumulative emissions cap but do not dependent on the year where we maximize the deviation. Finally, it is important to emphasize that the acquired depend on the optimization year. Moreover, in 3.2.4, it was shown that allowing the system to produce negative emissions does not drastically increase scenario-dependent deviationsare the extreme cases, not the plausible future realities. We conclude . This shows us that the carbon budget approach is robust to scenario choice under FaIR.

The second result of Sect. 3 is that the pulse response in the role of Green's function can indeed replicate the full-fledged generated scenario-dependent deviations to a great extent. Combined with the formal connection between the "perfect budget" and Green's approach, this implies that the pulse response shape can be used to indicate the source of the model 's associated same conclusion cannot be made for the one-box model. As was shown, the one-box model produces up to 10 times larger scenario-dependent deviations, which evolve in time but do not disappear. The reasons for the dramatically different generated deviations . The conclusion is that are explained in detail in Sect. 4.1 through the shape of the pulse response function. Essentially, if the model's pulse response shows a large degree of similarity to the FAIR model shows relatively small step function (dashed line, Fig. 1), i.e., if it peaks quickly, followed by a relaxation phase leading to a nearly constant value, the model will show small scenario-dependent deviations because its pulse responsereaches a close constant relatively fast as a result of its combination of temperature and carbon boxes' dynamics. In essence, we deduct that the pulse response's shape dictates scenario-dependent carbon budget deviations. Following the Looking at Fig. 1, one can see that FaIR is close to that behavior, while one-box is far from it. Joos et al. (2013) claim that having four carbon components and two temperature components is the minimum requirement to mimic this kind of pulse response. In climate economics, models often fail to meet this criterion. Besides the one-box model discussed here, the shape comparison of pulse responses presented by in Fig. 1 in Dietz et al. (2021) , we conclude shows that most simple climate models have some potential for carbon budget scenario dependency because of their inability to reach a constant temperature response – adding weight to the argument

[7] On the timescale of a human lifespan.

for replacing climate models with FaIR in integrated assessments ~~with FAIR. Dietz et al. (2021) argued that FAIR should be used in climate economics, referring to its pulse response representation being able to emulate the complex models' pulse response to justify it . Here, we connected the pulse response representation with the roots of~~ if carbon budget adherence is of importance (presumably, it is). Adherence to the carbon budget approach is especially important in the temperature target-based decision-making framework, as it is a crucial difference whether the temperature declines following emission cessation or is kept at the same level, as the carbon budget ~~and its deviations.~~ suggests. In the context of adhering to the temperature target, the declining temperature following emission cessation leads to non-intuitive policy recommendations, namely, to perpetually (albeit at a decreasing rate) continue emitting in order to adhere to the target.

~~Another finding comparing the optimization runs is an ever-increasing gap between the two approaches' generated temperatures with the increasing cumulative emissions. This effect occurs because we are restricted to using only one pulse responseas Green's function. Therefore, it cannot capture the state dependency as the full model with its non-linear processes. Nevertheless,~~ In this spirit, let us consider the connection between the ZEC metric and the pulse response. If ZEC is 0, as the ~~state-dependent effect can be detected when different pulse responses are generated under different climatic conditions. We have shown that~~ central estimate in MacDougall et al. (2020) suggests, this implies that temperature does not decrease or increase following the cessation of emissions. In the ~~pulse response decreases in magnitude and flattens with higher cumulative emissionsand temperatures. This finding in combination with a relatively flat shape of the~~ pulse response ~~function is used to generate a new, state-dependent carbon budget equation. The procedure is briefly reiterated as follows.~~

~~Since we have shown that FAIR-generated scenario dependencies are small and non-permanent, we approximate each of the (state-dependent) pulse responses with~~ context, this requires that the pulse response is a step function~~. Hence, we return to the "perfect budget" Green' s function case, but~~ , or close to it. Plotting the temperature leftover terms (Fig. 2) explicitly shows the two models' generated ZEC's under different climatic conditions (i.e., later in RCP run). Clearly, a model with a pulse response ~~step function that changes with~~ that does not show gradual relaxation (e.g. the one-box model) also shows a negative and declining ZEC. In contrast, FaIR produces a relatively small negative ZEC ($t_p = 2020, 2055, 2078$) that actually increases with changing climatic conditions, ~~de facto imitating a change of TCRE with every additional emission pulse. Finally, with the methodology explained in detail in Sect. 5, we derive a state-dependent carbon budget equation. Tested against the full-fledged model under the RCP scenarios, the new equation imitates the model almost perfectly for temperatures below 2.5 °C, when it starts to drift as a constant TCRE counterpart. The persistent,~~ becoming slightly positive in $t_p = 2100$. This raises the question as to whether ZEC itself is a state-dependent ~~deviation at the end of the century of RCP8.5 run is ~0.5 °C when using a constant TCRE, and ~0.1 °C when utilizing a state-dependent~~ value, i.e., whether the background climatic conditions dictate ZEC's value. This question is left to be explored in more advanced models.

Concluding that the carbon budget is indeed unaffected by emission scenario choice confirms the carbon budget approach's value as a tool for directly mapping cumulative emissions to temperature increase. However, the question remains as to the functional form of the carbon budget equation. ~~Since the full-fledged model shows the temperature anomaly of 3.4°C, the maximally achieved state-dependent deviation drops from around 30% to roughly 3% when switching from the constant (Eq. 1) to a state-dependent TCRE (Eq. 6). Additionally, the new proposed~~ Sect. 4 provides a clue as to how to deduct it from

the pulse response representation. Namely, if TCRE is a constant, the carbon budget equation ~~has an exponential form, which makes it very convenient for analytical assessments due to its functional properties. With its new, state-dependent form, we believe there is potential for~~ is linear. In Sect. 4, it was shown that the pulse response can be used as a proxy for TCRE, and that the pulse response decreases under changing climatic conditions in the default FaIR parametrization. A method was provided for deriving the non-linear carbon budget deviation from the changing pulse – a general method, which can be used for different models and different model calibrations. This offers an alternative approach to the ~~utilization of carbon budget approach in climate economics analytical assessments. Furthermore, what is genuinely surprising is that we have managed to capture the whole model with seven compartments into a single equation without losing too much precision.~~

~~In essence, this paper offers two ways to reformulate the~~ non-linear carbon budget equation derived in Nicholls et al. (2020), as it does not assume a functional form of the non-linear carbon budget ~~approach equation – Green's function formalism and the state-dependent carbon budget~~ equation ~~. One can recreate scenario-dependent effects, the other state-dependent drop of TCRE . The scenario-dependent effects are small, maximally around 7% of overall temperaturechange. Moreover, they are not constant in time due to the shape of the pulse response. On the other hand, state-dependent deviations are permanent, ever-increasing as a function of cumulative emissions, with a possible contribution to a drift of 30% from the full-fledged model's generated temperatures. Hence, tackling the state-dependency makes the state-dependent equation a likely candidate to substitute the full-fledged model in view of the~~ in advance, but derives it from TCRE dependency, building on Taylor expansion with respect to temperature, a key thermodynamic variable of the system investigated.

To address the lack of uncertainty in the analysis, Fig. 9 shows different pulse response representations for different FaIR calibrations. Following the methodology explained above, one can deduct that under different parameter sets, FaIR can mimic various levels of carbon budget non-linearity and even full linearity, while keeping scenario-independency robust, as TCRE, which approximates the corresponding pulse responses, can change its magnitude in either direction. This is possible because of the inclusion of both feedbacks on the carbon cycle and the temperature saturation, which counteract each other and can be tuned separately. Deriving the carbon budget equation explicitly for each calibration isn't pursued here, as doing so would not yield any new information and the set is too small to make generalized conclusions on e.g., how each FaIR parameter affects the carbon ~~budget approach.~~ budget. Among other questions raised, this is an interesting aspect for future research.

~~As an outlook for the follow-up research, we plan to thoroughly test the viability of the state-dependent equation. Firstly, the analysis ought to be redone so that the derived equation also includes the climate sensitivity or transient climate response parameter. This is crucial for sensitivity analyses which are essential in integrated assessments. Secondly, the equation is to be tested in some integrated assessment model which takes carbon only into account (e.g., MIND (Edenhofer et al., 2005)), and see how the objective function (e.g. welfare) changes if we replace the full climate model with one equation that does not include time-delay.~~

~~Conclusion~~

~~The current view of the carbon budgetapproach, if the aspiration is for it to be utilized in economic assessments, suffers from the inability to capture the emission scenario and climate state dependency. The latter causes more significant issues than the~~

former, as it causes a permanent deviation from the assumed budget under the cumulative emissions . Additionally, cumulative emissions is a monotonically increasing function, and so is a

6 Conclusion

This article focuses on deviations from the carbon budget approach, seen as a linear mapping from cumulative emissions and temperature increase, and draws a clear distinction between carbon budget emission scenario-dependent and climate state-dependent deviation. Conversely, the scenario dependency will primarily be affected by the model used or, more precisely, by the pulse response shape of the model used. In this paper, we reaffirmed the value of the FAIR climate model due to its simplicity and pulse response shape, which results in relatively small scenario-dependent deviations. Using that fact, we generated different pulse responses under different climatic conditions and approximated them with a Scenario-dependent deviations are the possible differences in resulting temperature that are solely due to the preceding emission choice, while the cumulative emissions of the preceding emission pathway remain fixed. In contrast, state-dependent deviations underline the change in TCRE value, which depends on the change of background climatic conditions – specifically, the cumulative emissions and global mean temperature increase. Importantly, state-dependent TCRE , which led to a fresh reformulation of the carbon budget approachleads to a non-linear carbon budget equation.

7 FAIR model

The Finite Amplitude Impulse-Response (FAIR) model was first introduced by Millar et al. (2017). In essence, it consists of the climate state-dependent modification to the carbon cycle of the simple climate-carbon cycle model proposed in Joos et al. (2013) , the latter of which does not include climate feedback . Following the FAIR introduction that consisted only of the carbon cycleand the associated radiative forcing, Smith et al. (2018) added the dynamics of other (non-CO_2) radiative forcers, hence introducing FAIRv1.3. The newest (to our knowledge) version of FAIR is published (FAIRv2.0.0) by Leach et al. (2021) . It incorporates the non-CO_2 dynamics from FAIRv1.3, but differs from the original in the way it represents the carbon feedback parameter and in the number of temperature boxes. Initially, FAIRv2.0.0 was introduced because of the more widely approachable feedback representation, which simplifies the pogramming scheme used for its employment. In GAMS, two representations are equivalent in programming difficulty level (as opposed to in, e.g. python). Nevertheless, in Section 2 introduces the reader to the FaIR, one-box and Green's function models. The FaIR model was chosen for the analysis for several reasons: Firstly, it has the ability to capture climate feedback on the carbon cycle; secondly, the model has already been praised in the literature for its efficiency; thirdly, it is relatively easy to implement and is computationally cheap; lastly, and most importantly for this paper, we use v2.0.0 as it is the most up-to-date FAIR version. it can accurately capture temperature response to the emission pulse (i.e., pulse response). The one-box model is introduced to study the effects of structural model uncertainty, as the model provides an example of a dramatically different pulse response representation. At its core, this paper

shows the implications of pulse response behavior on the carbon budget and its deviations, with the theory not restricted to the type of model under examination.

The FAIR model can be roughly divided into two modules, the carbon cycle module and the radiative forcing (temperature)module. Here, we provide a more detailed description of the model than in the main text, alongside a full set of equations and a complete utilized parameter values list. The following equations constitute the carbon cycle module:

$$\frac{\mathrm{d}R_i(t)}{\mathrm{d}t} = a_i E(t) - \frac{R_i(t)}{\alpha(t)\tau_i}, \; i = 1,2,3,4,$$

$$C(t) = C_0 + \sum_{i=1}^{4} R_i(t),$$

$$\alpha(t) = g_0 \cdot exp\left(\frac{r_0 + r_u G_u(t) + r_T T(t)}{g_1}\right),$$

$$G_u(t) = \sum_{s=t_0}^{t} E(s) - \sum_{i=1}^{4} R_i(t)$$

where, $g_1 = \sum_{i=1}^{4} a_i \tau_i \left[1 - (1 + 100/\tau_i)\,\mathrm{e}^{-100\mathrm{yr}/\tau_i}\right]$ and $g_0 = \exp\left(-\frac{\sum_{i=1}^{4} a_i \tau_i \left[1 - \mathrm{e}^{-100\mathrm{yr}/\tau_i}\right]}{g_1}\right)$. Four carbon compartments R_i constitute the carbon cycle, with each compartment being empty ($R_i = 0$) in preindustrial conditions. The total sum of the carbon content in the compartments in addition to the preindustrial concentration C_0 gives us the atmospheric carbon concentration $C(t)$ (Eq. (A2)). The carbon dynamics of the compartments R_i are given in Section 3 derives maximum scenario-dependent deviations using FaIR in its default parametrization, through an optimization program provided in Eq. (A14). The a_i fraction of emitted carbon $E(t)$ enters the ith compartment[8], while the content of the compartment decays with the rate of τ_i. The decay timescale is adjusted by the scaling factor $\alpha(t)$, which introduces the feedback mechanism in this model and hence effectively, the decay timescale at each timestep is given as a product of two ($\alpha(t)\tau_i$). Equation (A3) shows $\alpha(t)$ dependence on the global mean temperature $T(t)$ and the cumulative emissions taken up by the carbon sinks[8] $G_u(t)$ (Eq. (A4)). The intuition why we have such a dependence is given in the main text. Finally, from the carbon cycle module the atmospheric concentration $C(t)$ is extracted and translated into radiative forcing.

The radiative forcing part and the sequential warming dynamics are described with the following set of equations:

$$F(t) = f_1 \ln\frac{C(t)}{C_0} + f_2\left[\sqrt{C(t)} - \sqrt{C_0}\right],$$

[8] Nota bene, the emissions are usually given in units of GtC, while R_i is in ppm. Hence, $E(t)$ is divided by the conversion factor 2.12 in Eq. (A1). Conversely, $G_u(t)$ is counted in GtC

[8] Note that in the original form given by Leach et al, there is one added dependency on the gas atmospheric burden $G_a(t)$. However, if the analysis of methane is excluded in standard parametrization, the $\alpha(t)$ dependency on $G_a(t)$ equals zero.

$$\frac{dS_j(t)}{dt} = \frac{q_j F(t) - S_j(t)}{d_j},\ j = 1,2,3,$$

$$T(t) = \sum_{j=1}^{3} S_j(t).$$

First, the atmospheric concentration gives rise to the radiative forcing $F(t)$ through a combination of a logarithmic and square root term (optimization procedure tests the entire portfolio of emission scenarios and diagnoses those that produce extreme potential temperature differences under the same cumulative emissions. FaIR shows that the maximum possible scenario-dependent deviations are small compared to the total temperature increase and gradually diminish, confirming the carbon budget's robustness when it comes to scenario choice. It was also shown that, by using the model's pulse response as a Green's function in Eq. (A5)). Finally, 2), one can calculate the deviations with a correct order of magnitude. Hence, the forcing increases temperature as given by Eqs. A6 and A7. Following the similar structure as the carbon cycle, Equation A6 gives the temperature response of each box to radiative forcing, with the corresponding timescales d_j and parameters q_j that define the equilibrium temperature response . Finally, the global mean temperature anomaly $T(t)$ is calculated as the sum of three components in Eq. A7. Green's function approach offers a means of studying maximum possible scenario-dependent deviations in models of higher complexity and in a feasible computational time.

The first version of FAIR incorporates two temperature boxes, following the example set up by Geoffroy et al. (2013). Following the recent literature that suggests three box model is more appropriate to capture the behaviour observed in the state-of-the-art (CMIP6) climate models (Tsutsui (2020), Cummins et al. (2020)), Leach et al. (2021) introduce an additional (third) box to Section 4 shows that the FAIR temperature module. It might be worth noting that when we say compartments in this context we actually mean the modes of the compartments system after the diagonalization of the matrices that represent the actual carbon and temperature reservoirs and their correlated dynamic flows. This is why both atmospheric content and shape of the pulse response dictates scenario dependency. On the other hand, the change of pulse response with background climatic conditions can be reinterpreted as the state-dependent TCRE, which then leads to the temperature increase are the sum non-linear carbon budget equation. The method used to derive the carbon budget equation from pulse response, provided in Section 4, is universal and can be applied under different FaIR calibrations to see how individual climate drivers affect the non-linearity of the carbon and temperature "compartments". We stick to the nomenclature and do not name them modes in this work in order to follow the previous literature tradition.

The standard parameter values are as follows: the emission uptake fractions of each carbon reservoir $(a_1, a_2, a_3, a_4) = (0.217, 0.224, 0.28$ atmospheric decay timescales $(\tau_1, \tau_2, \tau_3, \tau_4) = (10^6, 394, 36.5, 4.3)$ yr; feedback parameters $(r_0, r_u, r_T) = (33.9, 0.0188\,\mathrm{GtC}^{-1}, 2.67\,^\circ\mathrm{C}^{-1})$ forcing coefficients $(f_1, f_2) = (4.57\,\mathrm{Wm}^{-2}, 0.086\,\mathrm{Wm}^{-2}\mathrm{GtC}^{-1/2})$, thermal response timescales $(d_1, d_2, d_3) = (0.903, 7.92, 355)$ yr; equilibrium responses $(q_1, q_2, q_3) = (0.18, 0.297, 0.386)\,^\circ\mathrm{CW}^{-1}\mathrm{m}^{-2}$. The final two sets of parameters (d_i and q_i) are tuned such that the model has a default value for equilibrium climate sensitivity equal to 3.24 K and transient climate response 1.79

Kbudget. This, in combination with employing more complex models' pulse responses as Green's functions, opens a promising avenue for further research.

Code and data availability. The codes and data sets used in this analysis can be found online on https://doi.org/10.5281/zenodo.8314808

Competing interests. The author has declared that there are no competing interests.

Acknowledgements. M. Bekchanov provided a GAMS-coded version of FAIR from Bekchanov et al. (2022). FaIR from Bekchanov et al. (2022). B. Blanz helped fixing the occurring fix certain code errors. V. Brovkin pointed out the paper in which the shape of the pulse response function was revealed (Joos et al., 2013). H. Held triggered this work , suggested inspecting the Green' set this work in motion, as he suggested examining Green's function directly from emissions to temperature , and to use and using the minimization and maximization operations to generate the folder of assess scenario dependence. I would also like to thank B. Blanz and H. Held for their helpful discussions. Lastly, I would like to thank H. Held for carefully reading the manuscript. This research was funded by the Deutsche Forschungsgemeinschaft (DFG, German Research Foundation) under Germany's Excellence Strategy – EXC 2037 'CLICCS - Climate, Climatic Change, and Society' – Project Number: 390683824.

References

Allen, M. R., Frame, D. J., Huntingford, C., Jones, C. D., Lowe, J. A., Meinshausen, M., and Meinshausen, N.: Warming caused by cumulative carbon emissions towards the trillionth tonne, Nature, 458, 1163–1166, publisher: Nature Publishing Group, 2009.

Allen, M. R., Friedlingstein, P., Girardin, C. A., Jenkins, S., Malhi, Y., Mitchell-Larson, E., Peters, G. P., and Rajamani, L.: Net zero: science, origins, and implications, Annual Review of Environment and Resources, 47, 849–887, 2022.

Bekchanov, M., Stein, L., Mohammadi Khabbazan, M., and Held, H.: Accuracy of subsidiary climate targets (concentration and cumulative emission) as substitutes to a temperature target: trade-offs between overshooting and economic loss, 2022.

Blau, R. A.: Stochastic programming and decision analysis: an apparent dilemma, Management Science, 21, 271–276, 1974.

Cummins, D. P., Stephenson, D. B., and Stott, P. A.: Optimal Estimation of Stochastic Energy Balance Model Parameters, Journal of Climate, 33, 7909–7926, https://doi.org/10.1175/JCLI-D-19-0589.1, publisher: American Meteorological Society Section: Journal of Climate, 2020.

Dietz, S. and Venmans, F.: Cumulative carbon emissions and economic policy: In search of general principles, Journal of Environmental Economics and Management, 96, 108–129, https://doi.org/10.1016/j.jeem.2019.04.003, 2019.

Dietz, S., van der Ploeg, F., Rezai, A., and Venmans, F.: Are Economists Getting Climate Dynamics Right and Does It Matter?, Journal of the Association of Environmental and Resource Economists, 8, 895–921, https://doi.org/10.1086/713977, publisher: The University of Chicago Press, 2021.

Edenhofer, O., Bauer, N., and Kriegler, E.: The impact of technological change on climate protection and welfare: Insights from the model MIND, Ecological Economics, 54, 277–292, https://doi.org/10.1016/j.ecolecon.2004.12.030, 2005.

Forster, P., Storelvmo, T., Armour, K., Collins, W., Dufresne, J.-L., Frame, D., Lunt, D., Mauritsen, T., Palmer, M., Watanabe, M., Wild, M., and Zhang, H.: The Earth's Energy Budget, Climate Feedbacks, and Climate Sensitivity Supplementary Material, in: Climate Change 2021: The Physical Science Basis. Contribution of Working Group I to the Sixth Assessment Report of the Intergovernmental Panel on Climate Change, edited by Masson-Delmotte, V., Zhai, P., Pirani, A., Connors, S. L., Péan, C., Berger, S., Caud, N., Chen, Y., Goldfarb, L., Gomis, M. I., Huang, M., Leitzell, K., Lonnoy, E., Matthews, J. B. R., Maycock, T. K., Waterfield, T., Yelekçi, O., Yu, R., and Zhou, B., book section 7, Cambridge University Press, Cambridge, UK and New York, NY, USA, https://www.ipcc.ch/report/ar6/wg1/downloads/report/IPCC_AR6_WGI_Chapter07_SM.pdf, 2021.

Geoffroy, O., Saint-Martin, D., Olivié, D. J. L., Voldoire, A., Bellon, G., and Tytéca, S.: Transient Climate Response in a Two-Layer Energy-Balance Model. Part I: Analytical Solution and Parameter Calibration Using CMIP5 AOGCM Experiments, Journal of Climate, 26, 1841–1857, https://doi.org/10.1175/JCLI-D-12-00195.1, publisher: American Meteorological Society Section: Journal of Climate, 2013.

Gillett, N. P., Arora, V. K., Matthews, D., and Allen, M. R.: Constraining the Ratio of Global Warming to Cumulative CO2 Emissions Using CMIP5 Simulations, Journal of Climate, 26, 6844–6858, https://doi.org/10.1175/JCLI-D-12-00476.1, publisher: American Meteorological Society Section: Journal of Climate, 2013.

Held, H.: Cost Risk Analysis: Dynamically Consistent Decision-Making under Climate Targets, Environmental and Resource Economics, 72, 247–261, https://doi.org/10.1007/s10640-018-0288-y, 2019.

IPCC: Climate Change 2014: Mitigation of Climate Change. Contribution of Working Group III to the Fifth Assessment Report of the Intergovernmental Panel on Climate Change, Cambridge University Press, Cambridge and New York, NY, 2014.

Joos, F., Roth, R., Fuglestvedt, J. S., Peters, G. P., Enting, I. G., Von Bloh, W., Brovkin, V., Burke, E. J., Eby, M., Edwards, N. R., et al.: Carbon dioxide and climate impulse response functions for the computation of greenhouse gas metrics: a multi-model analysis, Atmospheric Chemistry and Physics, 13, 2793–2825, 2013.

Khabbazan, M. M. and Held, H.: On the future role of the most parsimonious climate module in integrated assessment, Earth System Dynamics, 10, 135–155, 2019.

Lahn, B.: A history of the global carbon budget, WIREs Climate Change, 11, e636, https://doi.org/10.1002/wcc.636, _eprint: https://onlinelibrary.wiley.com/doi/pdf/10.1002/wcc.636, 2020.

Leach, N. J., Jenkins, S., Nicholls, Z., Smith, C. J., Lynch, J., Cain, M., Walsh, T., Wu, B., Tsutsui, J., and Allen, M. R.: FaIRv2.0.0: a generalized impulse response model for climate uncertainty and future scenario exploration, Geoscientific Model Development, 14, 3007–3036, https://doi.org/10.5194/gmd-14-3007-2021, publisher: Copernicus GmbH, 2021.

Leduc, M., Matthews, H. D., and Elía, R. d.: Quantifying the Limits of a Linear Temperature Response to Cumulative CO2 Emissions, Journal of Climate, 28, 9955–9968, https://doi.org/10.1175/JCLI-D-14-00500.1, publisher: American Meteorological Society Section: Journal of Climate, 2015.

MacDougall, A. H.: The oceanic origin of path-independent carbon budgets, Scientific Reports, 7, 10 373, 2017.

MacDougall, A. H. and Friedlingstein, P.: The origin and limits of the near proportionality between climate warming and cumulative CO2 emissions, Journal of Climate, 28, 4217–4230, 2015.

MacDougall, A. H., Frölicher, T. L., Jones, C. D., Rogelj, J., Matthews, H. D., Zickfeld, K., Arora, V. K., Barrett, N. J., Brovkin, V., Burger, F. A., et al.: Is there warming in the pipeline? A multi-model analysis of the Zero Emissions Commitment from CO 2, Biogeosciences, 17, 2987–3016, 2020.

Masson-Delmotte, V., Zhai, P., Pirani, A., Connors, S. L., Péan, C., Berger, S., Caud, N., Chen, Y., Goldfarb, L., Gomis, M. I., Huang, M., Leitzell, K., Lonnoy, E., Matthews, J. B. R., Maycock, T. K., Waterfield, T., Yelekçi, O., Yu, R., and Zhou, B., eds.: Summary for policymakers, pp. 3–32, Cambridge University Press, https://doi.org/10.1017/9781009157896.001, 2021.

Matthews, H. D. and Weaver, A. J.: Committed climate warming, Nature Geoscience, 3, 142–143, 2010.

Matthews, H. D., Gillett, N. P., Stott, P. A., and Zickfeld, K.: The proportionality of global warming to cumulative carbon emissions, Nature, 459, 829–832, https://doi.org/10.1038/nature08047, number: 7248 Publisher: Nature Publishing Group, 2009.

Meinshausen, M., Meinshausen, N., Hare, W., Raper, S. C. B., Frieler, K., Knutti, R., Frame, D. J., and Allen, M. R.: Greenhouse-gas emission targets for limiting global warming to 2 °C, Nature, 458, 1158–1162, https://doi.org/10.1038/nature08017, number: 7242 Publisher: Nature Publishing Group, 2009.

Millar, R., Allen, M., Rogelj, J., and Friedlingstein, P.: The cumulative carbon budget and its implications, Oxford Review of Economic Policy, 32, 323–342, https://doi.org/10.1093/oxrep/grw009, 2016.

Millar, R. J., Nicholls, Z. R., Friedlingstein, P., and Allen, M. R.: A modified impulse-response representation of the global near-surface air temperature and atmospheric concentration response to carbon dioxide emissions, Atmospheric Chemistry and Physics, 17, 7213–7228, https://doi.org/10.5194/acp-17-7213-2017, publisher: Copernicus GmbH, 2017.

Nicholls, Z.: Reduced Complexity Model Intercomparison Project (RCMIP), pp. EGU21–3707, https://doi.org/10.5194/egusphere-egu21-3707, conference Name: EGU General Assembly Conference Abstracts ADS Bibcode: 2021EGUGA..23.3707N, 2021.

Nicholls, Z., Gieseke, R., Lewis, J., Nauels, A., and Meinshausen, M.: Implications of non-linearities between cumulative CO2 emissions and CO2-induced warming for assessing the remaining carbon budget, Environmental Research Letters, 15, 074 017, 2020.

Peters, G. P.: Beyond carbon budgets, Nature Geoscience, 11, 378–380, https://doi.org/10.1038/s41561-018-0142-4, number: 6 Publisher: Nature Publishing Group, 2018.

Petschel-Held, G., Schellnhuber, H.-J., Bruckner, T., Toth, F. L., and Hasselmann, K.: The tolerable windows approach: theoretical and methodological foundations, Climatic Change, 41, 303–331, 1999.

Raupach, M. R.: The exponential eigenmodes of the carbon-climate system, and their implications for ratios of responses to forcings, Earth System Dynamics, 4, 31–49, https://doi.org/10.5194/esd-4-31-2013, 2013.

Ricke, K. L. and Caldeira, K.: Maximum warming occurs about one decade after a carbon dioxide emission, Environmental Research Letters, 9, 124 002, 2014.

Rogelj, J., Shindell, D., Jiang, K., Fifita, S., Forster, P., Ginzburg, V., Handa, C., Kheshgi, H., Kobayashi, S., Kriegler, E., et al.: Mitigation pathways compatible with 1.5 C in the context of sustainable development, in: Global warming of 1.5 C, pp. 93–174, Intergovernmental Panel on Climate Change, 2018.

Shine, K. P., Fuglestvedt, J. S., Hailemariam, K., and Stuber, N.: Alternatives to the global warming potential for comparing climate impacts of emissions of greenhouse gases, Climatic change, 68, 281–302, 2005.

Shukla, P. R., Skea, J., Slade, R., Al Khourdajie, A., Van Diemen, R., McCollum, D., Pathak, M., Some, S., Vyas, P., Fradera, R., et al.: Climate change 2022: Mitigation of climate change, Contribution of working group III to the sixth assessment report of the Intergovernmental Panel on Climate Change, 10, 9781009157926, 2022.

Smith, C. J., Forster, P. M., Allen, M., Leach, N., Millar, R. J., Passerello, G. A., and Regayre, L. A.: FAIR v1.3: a simple emissions-based impulse response and carbon cycle model, Geoscientific Model Development, 11, 2273–2297, https://doi.org/10.5194/gmd-11-2273-2018, publisher: Copernicus GmbH, 2018.

Stocker, T. F., Qin, D., Plattner, G.-K., Tignor, M., Allen, S. K., Doschung, J., Nauels, A., Xia, Y., Bex, V., and Midgley, P. M., eds.: Summary for policymakers, pp. 3–29, Cambridge University Press, Cambridge, UK, https://doi.org/10.1017/CBO9781107415324.004, 2013.

Traeger, C. P.: ACE – Analytic Climate Economy, SSRN Electronic Journal, https://doi.org/10.2139/ssrn.3832722, 2021.

Tsutsui, J.: Diagnosing Transient Response to CO2 Forcing in Coupled Atmosphere-Ocean Model Experiments Using a Climate Model Emulator, Geophysical Research Letters, 47, e2019GL085844, https://doi.org/10.1029/2019GL085844, _eprint: https://onlinelibrary.wiley.com/doi/pdf/10.1029/2019GL085844, 2020.

Zickfeld, K., Eby, M., Matthews, H. D., and Weaver, A. J.: Setting cumulative emissions targets to reduce the risk of dangerous climate change, Proceedings of the National Academy of Sciences, 106, 16 129–16 134, https://doi.org/10.1073/pnas.0805800106, publisher: Proceedings of the National Academy of Sciences, 2009.